MICROCOPY RESOLUTION TEST CHART
NATIONAL BUREAU OF STANDARDS 1963

ER-7814-2

(12) 6

INHIBITION
OF
HYDROGEN EMBRITTLEMENT
IN
HIGH STRENGTH STEEL

By

C. S. KORTOVICH

TECHNICAL REPORT

Prepared for
Office of Naval Research
Contract N00014-74C-0365

349550

FEBRUARY 1977

D D C
RECEIVED
MAR 25 1977
A

TRW

EQUIPMENT
MATERIALS TECHNOLOGY

TRW-ER-7814-2

TECHNICAL REPORT

INHIBITION OF HYDROGEN EMBRITTLEMENT IN HIGH STRENGTH STEEL

Prepared for

48p.

Feb 77

C. S. Kortovich

TRW Inc.
TRW Equipment
Materials Technology
Cleveland, Ohio 44117

349 550

FOREWORD

The work described in this report was performed under sponsorship of the Office of Naval Research, Contract N00014-74-C-0365 with Dr. P. A. Clarkin acting as Program Manager for the Navy. Work conducted during the first year of this contract involved a study of the effect of rare earth additions on the hydrogen embrittlement resistance of cathodically charged and cadmium plated 4340 steel. Work conducted during the second year, covered in this report, concluded the efforts involving charged and plated 4340 steel.

This report has been assigned TRW Equipment Number ER 7814-2 and the data are reported in laboratory notebooks Nos. 605 and 794.

i

ABSTRACT

The addition of rare earth gettering agents to trap hydrogen was evaluated as a method of reducing the embrittlement problems in steel cathodically charged with hydrogen. Additions of lanthanum and cerium made to AISI 4340 steel were used in the 0.03-0.17 weight percent range.

Mechanical property results were comparable for both elements and indicated that while some degradation in property levels occurred, particularly at the high rare earth content, most of the aircraft quality specification minimums for 4340 high strength steel were attained. An important exception was the Charpy impact strength, which was approximately 15% below the minimum. Property loss was attributed to the formation of continuous rare earth oxide inclusions at prior austenite grain boundaries.

Delayed failure test results indicated substantial improvements in hydrogen embrittlement resistance for high rare earth content (>0.15 weight percent) steels. This was manifested in terms of increased time to crack initiation (incubation time), increased failure time, higher values for the lower critical stress intensity and lower crack growth rates compared to baseline 4340 or the low rare earth modifications. Cerium was slightly superior to lanthanum only in terms of resulting in a higher level for the lower critical stress intensity.

TABLE OF CONTENTS

I   INTRODUCTION

The deleterious effects resulting from hydrogen in ferrous materials have been known since 1926, when ductility losses in steels were attributed to the presence of hydrogen in the materials (1,2). The magnitude of the hydrogen problem, however, has come to be appreciated in the last twenty-five years primarily because of the increasing demands for strength and toughness required of modern materials exposed to hydrogen environments.

The earliest recognized and most extensively studied form of hydrogen embrittlement of high strength steel is that due to hydrogen within the metal lattice (3-6). Hydrogen can be introduced into a metal by a variety of industrial processes such as welding, acid pickling and electroplating resulting in a high hydrogen concentration gradient at the metal surface (7-11). Hydrogen embrittlement has also been observed in steel structural components exposed to aqueous environments (12). Termed stress corrosion cracking, this natural process can result in the failure of a component from the combined action of stress and chemical attack. It is now fairly well established that stress corrosion cracking of steels in aqueous solutions is governed, at least to some extent, by a series of electrochemical reactions at the surface which permit the entry of hydrogen into the metal (13). The most recent type of hydrogen embrittlement to be investigated results from the direct exposure of a metal surface to a gaseous hydrogen environment (14,15). This form of hydrogen embrittlement has been regarded with increasing concern because of the predicted future widespread use of a hydrogen as a fuel (5). Absorption of hydrogen gas in metals is potentially a serious problem for electric current generating fuel cells and propulsion systems which utilize the hydrogen-oxygen reaction as a source of energy (16,17) or for systems being considered for the storage of high pressure gaseous hydrogen fuel (18).

The general effect of hydrogen is to decrease the strength of a component causing failure to occur at stress levels below those normally used for design criteria. Because of this, considerable effort has been devoted to both the characterization of the phenomenological aspects of hydrogen embrittlement and the methods to eliminate or minimize the problem. Studies have focused on three important areas: (1) the original location and form of hydrogen, (2) the transport reactions involved in the movement of hydrogen from its origin to some point where it can interact with the metal lattice to cause embrittlement, and (3) the mechanisms of the embrittlement interactions. Although an appreciable understanding of the effects of hydrogen on high strength steels has been achieved, and some progress has been made in mitigating the embrittlement problem, the fact still remains that design engineers must incorporate considerable safety factors to insure the prevention of catastrophic failure in structural steel components.

The three general areas in which efforts have been made to minimize the effect of hydrogen in high strength steels include the following: (1) within a component itself, where hydrogen can be trapped and rendered less harmful, the embrittlement mechanism altered or the hydrogen movement process retarded, (2) the interface between the component and the service environment, where a barrier to hydrogen entry can be formed, and (3) the environment, where in certain applications enough flexibility exists to modify the system such that the reaction rates controlling hydrogen entry can be appreciably minimized.

Several techniques have shown promise in influencing the degree of embrittlement once hydrogen has entered the component including microstructural and chemistry alterations (19-21), baking (22-24) and prestressing (25-27). A number of serious limitations exist with the application of these methods. For microstructure and base alloy composition modifications, overall mechanical property, fabricability and economic considerations control the applicability of such methods to the extent that little real flexibility exists for wide variations without other accompanying problems. For baking, long bake times are impractical and expensive and elevated bake temperatures are seriously limited because of the potential degradation of base metal properties. For prestress techniques, the major disadvantage is that controlled amounts of the required magnitude of stress may be difficult to impart, particularly to components of complex shape.

Numerous methods have been studied to prevent hydrogen entry into a high strength steel component by the formation of a barrier between the steel and the service environment. Metallic platings have been developed for the protection of steels, but there has been an accompanying embrittling action resulting from the plating process itself (28-31). Other methods employed to form a protective surface interface include cathodic protection (32,33), nonmetallic coatings (34,35) and heat treatments utilized to promote a selective surface composition change resistant to hydrogen entry (36). Cathodic protection of steels can be limited by the absorption of hydrogen generated at the cathodic surfaces if high local current densities are applied. Nonmetallic coatings are limited in their application because of their susceptibility to foreign object damage and thermal shock. Selective surface composition changes are somewhat limited because of the heterogeneous nature of the changes themselves.

The most restricted of the inhibition techniques, modification of the embrittling environment, suffers from the fact that a structural component's service environment cannot always be altered. The most immediate applications for these methods would be steel tubing or pressure vessels which contain or transfer hydrogen containing fluids or gasses (37-39). In general, however, these techniques cannot always be applied.

2

Because of these limitations research is being conducted to improve current methods and to develop new ones to inhibit hydrogen embrittlement to high strength steels. One method is the use of rare earth additions. Historically, rare earth additions such as lanthanum and cerium have been made in the range .05-.15 w/o for sulfide shape control (40,41). Although strong deoxidizers, their addition after standard aluminum deoxidation practice has resulted in desulfurization (41) and a change in manganese sulfide shape from long parallel rods to a spherical or globular form (40,42). Increases in impact strength and enhanced isotropy of mechanical properties have been reported for steels with such inclusion morphology (43). Other investigators have reported increases in hardness, tensile strength and elongation as well as impact strength with rare earth additions (44). Lanthanum and cerium in particular have resulted in reduced sensitivity of temper embrittlement and a shift in the embrittlement range towards lower temperatures (45).

Recent studies have indicated that rare earth additions to high strength steels can also increase their resistance to hydrogen embrittlement. Cerium and lanthanum appear particularly promising in this regard. Cerium additions at the 0.2 w/o level in 4340 type steels have resulted in lower susceptibility to the blister or flake formation type of hydrogen embrittlement by forming stable hydrides below 1850°F (1010°C) (46). Additions at the 0.07 level were also found to improve corrosion resistance of cast irons in 5% aqueous sulphuric acid solutions by modifying the flake graphite morphology to a nodular form (47). Additions of cerium and lanthanum in combination (approximately 60%Ce, 40%La) added at the 0.05, 0.09 and 0.13 w/o levels to HY-80 steel decreased the susceptibility of weldments made from this material to hydrogen-induced cracking (48). There appeared to be an optimum concentration of rare earths (0.09 w/o) to achieve the maximum reduction in susceptibility to the hydrogen induced cracking. The improvement was related to the effect of the rare earth additions on the morphology of the sulfides formed in that the change from an elongated particle to a spherical particle morphology significantly reduced the sensitivity of the weldments to hydrogen-induced cracking. It was suggested that the modification of the sulfide compositions may also have been a contributing factor to the improvement, but further studies were suggested as necessary to establish this fact. In another welding study, the addition of 0.2 w/o Misch Metal (50% cerium plus lanthanum and other rare earths) was able to eliminate diffusible hydrogen in HY-130 weldments by the formation of stable hydrides (49).

These studies indicate that rare earth additions to high strength steels offer potential to minimize hydrogen embrittlement without degrading the baseline properties of the alloys themselves. The important consideration here is the mechanism by which rare earths minimize embrittlement. In one instance (46), improvement was attributed to the absorption of hydrogen to form stable, nonembrittling hydrides. In another instance (48), improvement was attributed to a change in sulfide morphology. An additional important consideration is the amount of rare earth additions required to inhibit hydrogen embrittlement. It is well established that embrittlement results from hydrogen

contents as low as 10 ppm (50). Enough rare earth must be in the alloy system to provide improvement in resistance to hydrogen embrittlement without causing a significant alteration in the mechanical properties of the base alloy itself. Fabricability and workability of alloy systems containing these rare earths are also important factors in determining their potential use.

The purpose of the current study was to develop a method to minimize the effect of hydrogen embrittlement in high strength steels through the addition of rare earths. Specifically, efforts were concentrated on cerium and lanthanum additions made to AISI 4340 steel plates. The experimental approach involved first a determination of the effect of various amounts of these rare earths on the baseline mechanical properties including room temperature tensile and Charpy impact tests. Resistance to hydrogen embrittlement was then characterized in terms of delayed failure tests conducted on specimens cathodically charged in sulfuric acid and cadmium plated. The results were analyzed to determine which element had the greatest potential to improve the hydrogen embrittlement resistance of 4340 steel.

II   MATERIALS AND PROCEDURES

Six experimental heats of AISI 4340 were used for this study. Material was received in the form of 3/4" (1.9 cm) thick plates. The processing operations for this material consisted of first making 50 pound (22.6 Kg) aluminum deoxidized vacuum induction melted ingots 4 3/4" (13.1cm) x 4" (10.0 cm) x 10" (25.4 cm) which were then forged and crossrolled to final shape. Forging and cross-rolling were conducted at 2150°F (1066°C) in 5 passes to obtain a final product 3/4" (1.9 cm) x 8-1/2" (21.6 cm) x 20" (51 cm). The material was then annealed at 1150°F (621°C) for 8 hours. This ingot breakdown procedure is representative of typical operations conducted within the steelmaking industry for 4340 and as such clearly demonstrated the workability of 4340 steel made with the level of rare earth additions studied in this program.

The compositions for these heats are listed in weight percent (w/o) in Table I. All standard elements fell within the specifications for AISI 4340. It was noted, however, that the heats designed to contain 0.1 and 0.2 w/o lanthanum also contained certain amounts of cerium. This was due to the fact that the lanthanum silicide used to make the rare earth addition also contained cerium and the level of cerium recovery was much higher than expected.

All test material was heat treated prior to finish machining according to the following sequence:

1.   Normalize 15 minutes, salt bath at 1700°F (927°C), air cool.

2.   Austenitize 30 minutes, salt bath at 1550°F (843°C), oil quench.

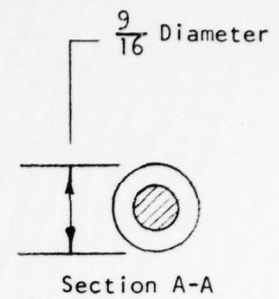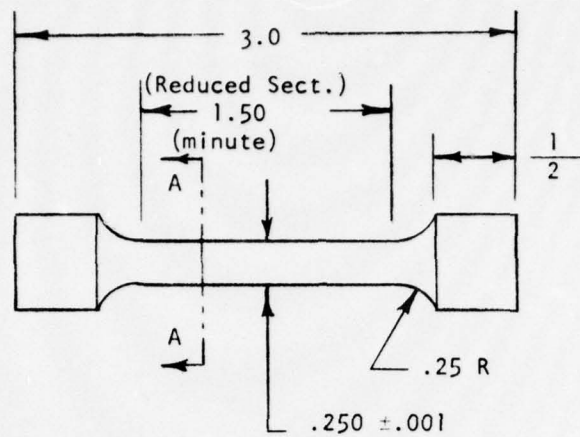3.   Temper in air, 1 hour plus 1 hour at 450°F (232°C), air cool.

The 450°F (232°C) tempering temperature was selected because of the resultant high strength of the 4340 and its increased sensitivity to hydrogen embrittlement (51).

Delayed failure testing of hydrogenated and plated specimens was utilized to determine the ability of rare earth additions to inhibit hydrogen embrittlement. Prior to delayed failure testing, however, mechanical property characterizations were conducted to determine the effects of the rare earth additions themselves on the uncharged baseline material and the possible embrittling behavior of their hydrides on hydrogen charged material. Evaluations included duplicate room temperature tensile and Charpy impact tests performed on charged and uncharged specimens having the configurations shown in Figure 1. Hydrogen was introduced electrolytically into the specimens with a charging condition selected to insure that a condition of irreversible (i.e., severe) embrittlement existed (52). The procedure involved degreasing specimens in acetone followed by cathodic charging for 30 minutes in a 4% sulfuric acid solution at
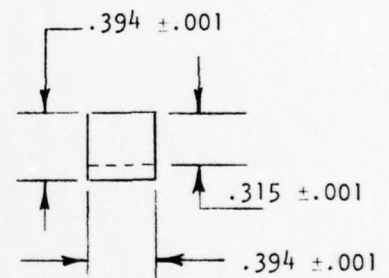
Table I

Composition of 4340 Heats in w/o

Heat	Nominal Rare Earth Addition	C	Mn	P	Si	Ni	Cr	Mo	Al	Ce	La	O_2	N_2	S	Fe
X409	None	.39	.71	.008	.20	1.77	.82	.24	.047	-	-	.004	.001	.004	Balance
X410	0.05 w/o Ce	.41	.68	.008	.28	1.79	.78	.23	.055	.033	-	.002	.001	.004	"
X411	0.1 w/o Ce	.41	.68	.005	.28	1.81	.83	.23	.048	.092	-	.002	.001	.004	"
X421	0.2 w/o Ce	.40	.76	.008	.34	1.80	.88	.26	.087	.17	.015	.001	.001	.004	"
X412	0.1 w/o La	.41	.78	.005	.28	1.81	.88	.23	.055	.054	.078	.003	.001	.004	"
X422	0.2 W.o La	.40	.75	.008	.31	1.74	.85	.27	.056	.028	.16	.001	.002	.008	"
AISI	4340 Spec.	.38/.43	.60/.80	.04(Max)	.20/.35	1.65/2.00	.70/.90	.20/.30	-	-	-	-	-	.04(Max)	"

3.0

(Reduced Sect.)
1.50
(minute)

A

A

.25 R

.250 ±.001

$\frac{1}{2}$

$\frac{9}{16}$ Diameter

Section A-A

a) Tensile Test Specimen Configuration

2.165 ±.010

1.082

+.001
-.000
.010 Rad.

Bottom of Notch
Must be Lapped

±1°

45°

.394 ±.001

.315 ±.001

.394 ±.001
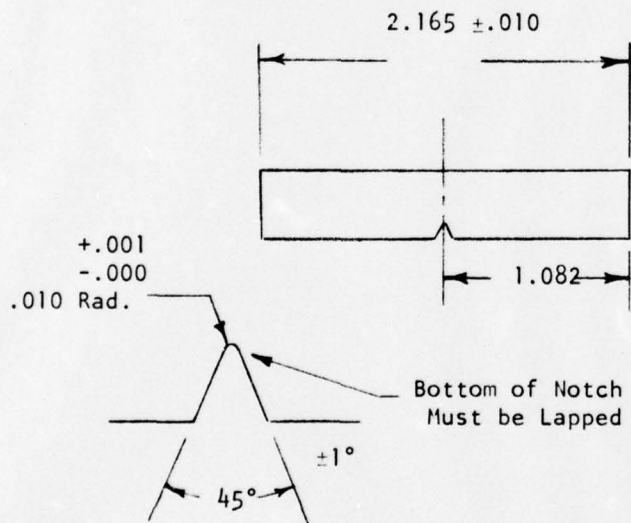
b) Charpy Impact Test Specimen Configuration

Figure 1. Schematic illustration of tensile and Charpy impact specimen
configurations used for mechanical property characterization
study. All dimensions are in inches.

7

a current density of 0.02 amp/in^2 (0.003 amp/cm^2). Following charging, the specimens were rinsed in distilled water and cadmium plated in a sodium cyanide cadmium oxide bath containing organic brightners for 15 minutes at a current density of 0.14 amp/in^2 (0.022 amp/cm^2). In order to homogenize the resulting hydrogen distribution, the specimens were baked for 30 minutes at 300°F (149°C) in air. Previous work had indicated that this treatment effectively eliminates the hydrogen gradient produced by charging (53).

The delayed failure tests were conducted on precracked compact K$_{Ic}$ plate specimens 0.5" (1.27 cm) thick having the configuration shown in Figure 2a. The specimen orientation for these, as well as the tensile and Charpy impact test specimens are shown in Figure 2b, and represent the long transverse direction. To facilitate the formation of a fatigue precrack, an EDM slot was placed at the root of the machined notch 0.050" (1.27 mm) deep and 0.010" (.254 mm) thick. Precracking was then performed after heat treatment on an SF-1U Sonntag fatigue machine at stresses which provided the desired crack length, 0.6" (1.52 cm), in 40-50,000 cycles. After precracking, the specimens were cleaned with acetone, hydrogenated and plated according to procedures described previously for the mechanical property test specimens. Tests were performed on constant load, self-leveling, lever-loaded Satec creep rupture machines. Crack growth kinetics were determined with a 350 OHM Bridge Fracture Roughness Clip Gauge Transducer which recorded changes in the specimen compliance. After conversion from compliance to crack length, these length values were plotted as a function of time and slopes (da/dt) were obtained at various values of crack length and plotted versus the instantaneous stress intensity at the crack tip. Light and scanning electron microscopy and electron microprobe analysis was used on selected specimens to determine the effect of the rare earth additions on the general microstructue and in particular the crack propagation paths.

a) Precracked Compact K_{Ic} Plate Specimen Configuration

W = 1.0"
A = 0.35"
B = 0.50"

b) Specimen Orientation

Figure 2. Precracked compact K_{Ic} plate specimen configuration and overall orientation used for the present study.

III RESULTS AND DISCUSSION

The overall objective of this program was to develop a method to inhibit the effect of hydrogen embrittlement in high strength steels. At present the current inhibition methods are limited in terms of overall effectiveness and are usually applied only to specific steels for certain applications. Rare earth additions, however, have shown promise as a means to increase the resistance of high strength steels to hydrogen embrittlement. In the current study efforts were concentrated on cerium and lanthanum additions made to AISI 4340 steel. First a determination was made of the effect of various amounts of these rare earths on the baseline mechanical properties. Resistance to hydrogen embrittlement was then characterized in terms of delayed failure tests conducted on specimens cathodically charged in sulfuric acid and cadmium plated.

A. Mechanical Property Characterization

1. Room Temperature Tensile Results

The results of the room temperature tensile tests for both uncharged and charged material are listed in Table II and the data are plotted in Figures 3 and 4 as a function of weight percent (w/o) rare earth. For ultimate and 0.2% yield strength, Figure 3, a maximum occurred in the range .08-.09 w/o for both rare additions. This strengthening behavior as a result of rare earth additions has been well established for ferrous alloys and has been attributed to the deoxidizing and desulfurizing action of the rare earths and to the resultant change in sulfide morphology (54,43). As shown in Figures 5 and 6, however, the addition of greater amounts of rare earths than normally used in the steel industry (0.1 w/o) resulted in massive and continuous grain boundary inclusions in these specimens. Electron microprobe analysis indicated that in the case of the baseline alloy inclusions were predominantly manganese and zirconium rich oxysulfides, while in the case of the rare earth alloys the inclusions were primarily rich in cerium, iron, and oxygen or lanthanum, iron and oxygen depending upon which rare earth was added to the 4340. An example of these microprobe results are shown in Figure 7 for Heat X421 (0.17 w/oCe). In spite of the fact that the continuous inclusions offered ideal paths for crack propagation, there was only a slight decrease in strength properties compared to the baseline material. For example, at the 0.16-0.17 w/o level, a decrease of 2.3% (Ce) - 3.5% (La) was observed in ultimate tensile strength, while a decrease of 1.9% (Ce) -3.5% (La) was observed in 0.2% offset yield strength.

While the strength properties of the cerium modified 4340 were slightly superior to those of the lanthanum modified steel, the overall effect was not significant. The maximum difference in ultimate tensile strength was 1.0% while the maximum difference in 0.2% offset yield strength was 1.6%, both occurring at the highest rare earth level. Tests were also conducted on hydrogen charged and cadmium plated specimens to determine the possible

10

Table II

Room Temperature Tensile Results for Rare Earth
Modified AISI 4340 Steel

Heat	Alloy	Test Condition	Ultimate Tensile Strength		0.2% Offset Yield Strength		% Elongation	% Reduction Area
			KSI	MN/m^2	KSI	MN/m^2		
X409	Base 4340	Uncharged	253.9	1750.2	206.2	1421.4	13.3	50.4
		Charged	253.3	1746.1	203.8	1405.5	12.8	50.1
X410	4340+.03Ce	Uncharged	256.7	1769.8	205.0	1413.0	13.0	45.9
		Charged	258.1	1779.1	208.9	1440.2	12.3	43.1
X411	4340+.09Ce	Uncharged	260.8	1798.5	209.9	1447.2	9.0	32.3
		Charged	261.1	1800.7	213.5	1472.4	10.5	35.1
X421	4340+.17Ce	Uncharged	247.9	1709.2	199.6	1376.1	10.3	34.7
		Charged	247.1	1703.7	202.9	1399.2	10.0	33.1
X412	4340+.08La	Uncharged	259.3	1788.1	207.6	1431.1	12.3	40.7
		Charged	258.3	1781.1	211.1	1455.7	11.0	43.0
X422	4340+.16La	Uncharged	245.4	1691.8	196.5	1354.4	8.0	27.9
		Charged	245.0	1689.0	198.5	1368.4	9.5	35.4

Figure 3. Room temperature ultimate and 0.2% offset yield strength results plotted as a function of rare earth content in AISI 4340 steel.
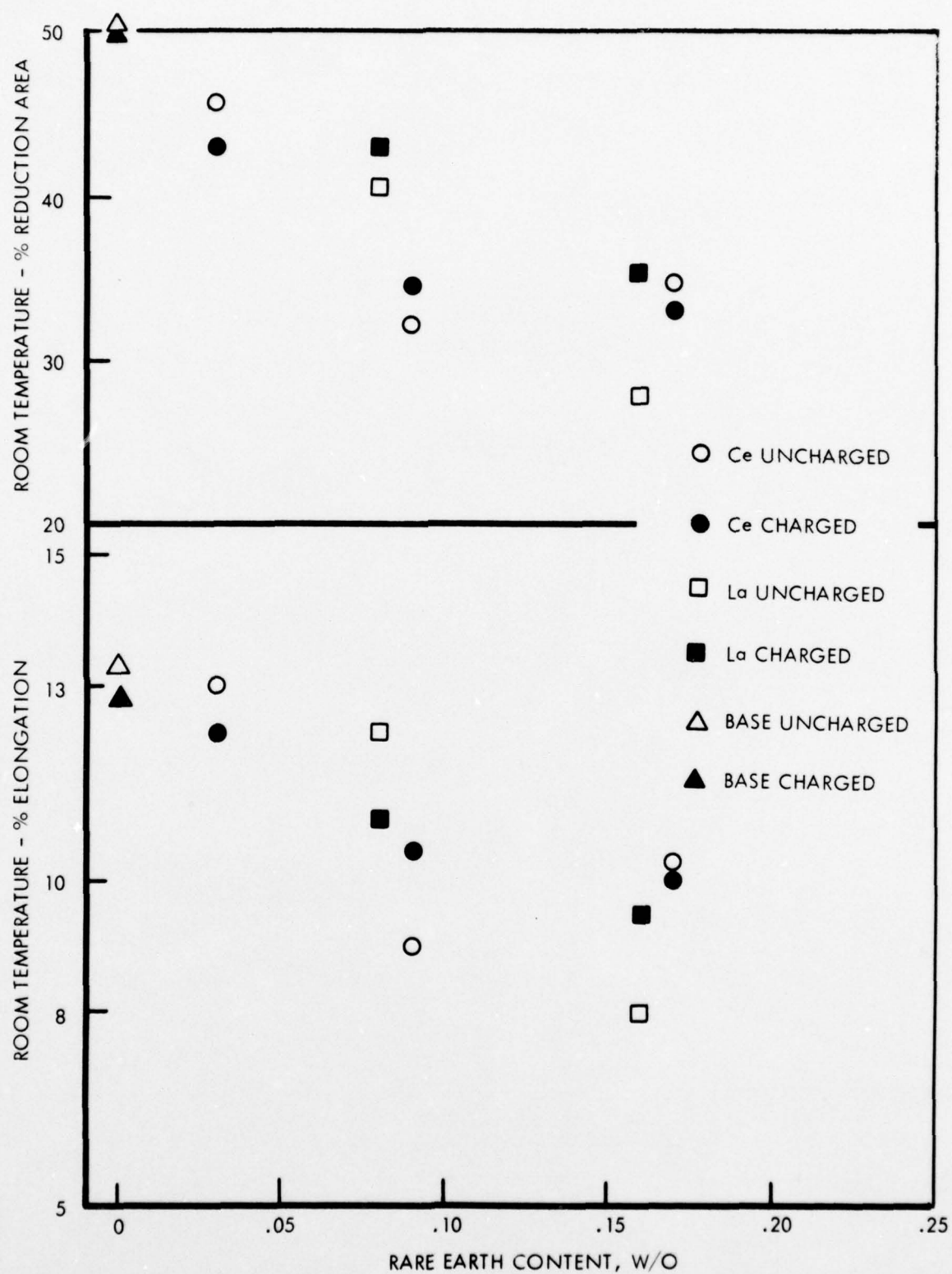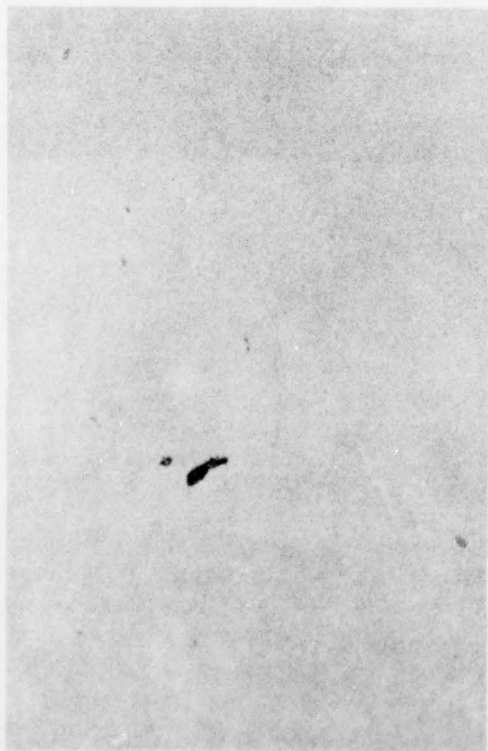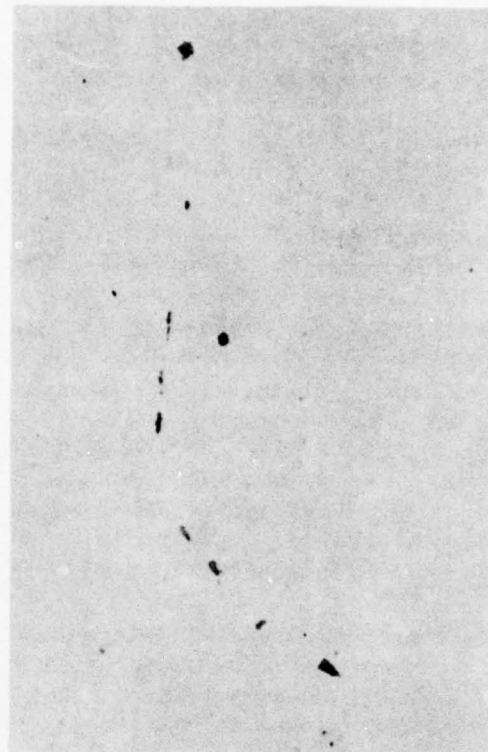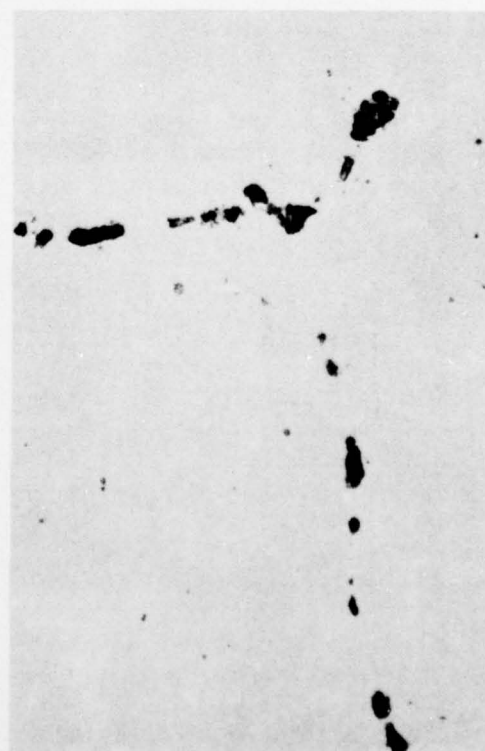
Figure 4. Room temperature percent elongation and reduction of area results plotted as a function of rare earth content in AISI 4340 steel.
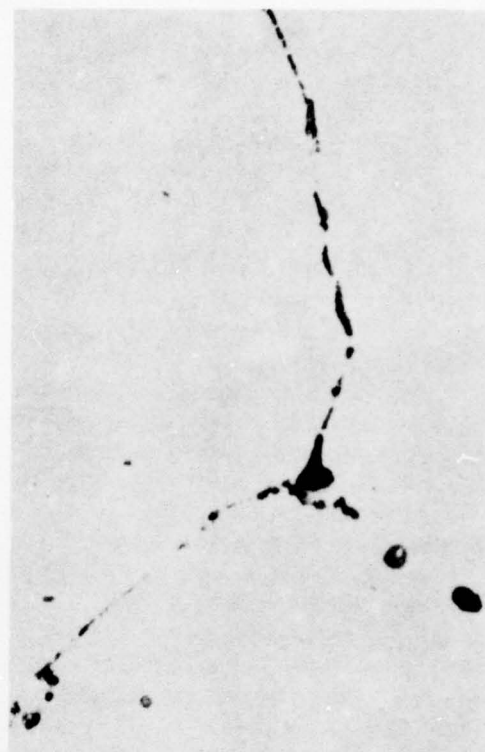
a) Heat X409 - No Rare Earth Additions

b) Heat X410 - .033 w/o Cerium

c) Heat X411 - .092 w/o Cerium

d) Heat X421 - .170 w/o Cerium

Figure 5.   Light photomicrographs of base and cerium rare earth modified AISI 4340 steel. Unetched. 500X Magnification.
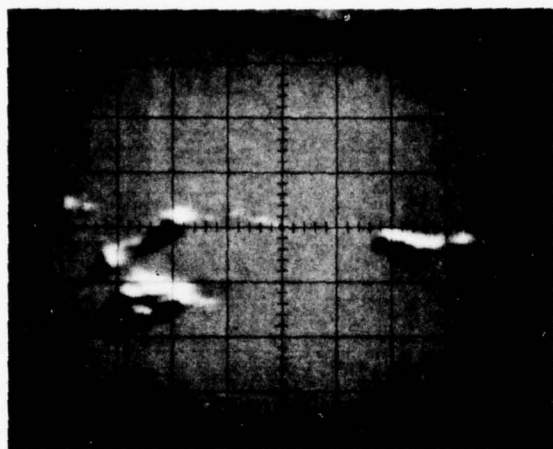
14

a) Heat X412 - .078 w/o Lanthanum

b) Heat X422 - .160 w/o Lanthanum

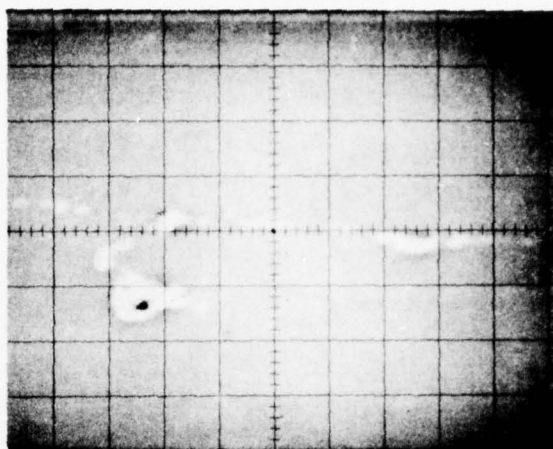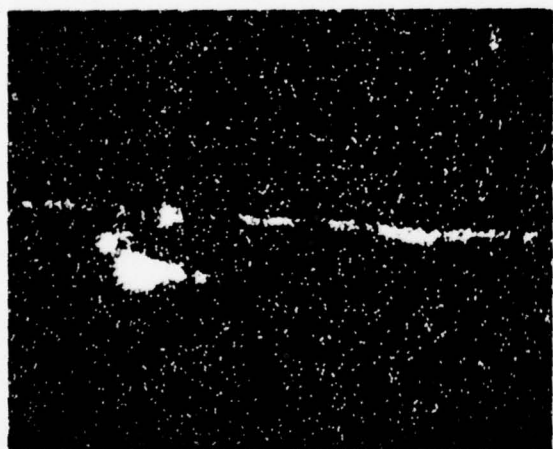Figure 6. Light photomicrographs of lanthanum modified AISI 4340
steel. Unetched. 500X Magnification.

a) Back Scatterred Current Image

b) Absorbed Current Image

c) Cerium X-ray Pattern

d) Oxygen X-ray Pattern

Figure 7. Electron microprobe photomicrographs for Heat X421 (0.17 w/o Ce) showing back scattered and absorbed current images and cerium and oxygen X-ray patterns at 800X magnification.

embrittling effect of any rare earth hydrides formed. Comparison with the results for uncharged material indicated little significant effect. The ultimate tensile strength values were comparable while the 0.2% yield strengths were approximately 0.8-1.7% higher for the charged material.

The room temperature percent elongation and percent reduction of area results are plotted in Figure 4 and indicate a decrease with the addition of both cerium and lanthanum. While maxima have been observed in the ductility properties of rare earth modified high strength steels, these have usually occurred at much lower rare earth levels than used in the present study (i.e., 0.01-0.02 w/o) (54).

In the present study the greatest ductility loss was obtained at the high rare earth level. For example, at 0.16-0.17 w/o, a decrease of 22.6% (Ce) - 39.8% (La) was observed in percent elongation, while a decrease of 31.1% (Ce) - 44.6% (La) was observed in the percent reduction of area. In spite of this ductility loss, however, only the lanthanum modified 4340 would not have met the required ductility specifications for Aircraft Quality 4340 in the 450°F (232°C) - 475°F (246°C) temper condition (transverse percent elongation 6% minimum, transverse percent reduction of area 25% minimum - 30% average) (55). The ductility loss in these steels was attributed to the formation of massive and continuous grain boundary inclusions which offered ideal paths for crack propagation.

Comparison of the ductility results for uncharged and hydrogen charged material indicated only that hydrogen charging produced no serious degrading effect upon the properties. Some inconsistency was observed in the data, however. In the case of cerium, charged material at the 0.09 w/o level had higher reduction of area values than uncharged material, while at the 0.17 w/o level the reverse was true. Similar results were obtained for percent elongation. In the case of lanthanum, charged material at the 0.08 w/o level had lower reduction of area values than uncharged material, while at the 0.16 w/o level the reverse was true.

2. Room Temperature Charpy Impact Results

The results of the room temperature Charpy impact tests for both uncharged and charged material are listed in Table III and the data are plotted in Figure 8 as a function of w/o rare earth. Comparison with the baseline value indicated a sharp decrease as rare earth content increased. At the 0.16-0.17 w/o level, a decrease of approximately 53% in Charpy impact strength was observed for both the cerium and lanthanum modified steels. These values were approximately 15% below the 13.0 ft-lb specification for Aircraft Quality 4340 in this temper condition (55) and reflect the embrittling nature of the continuous grain boundary inclusions formed at the high rare earth levels. Studies have been conducted on the effects of rare earth additions on impact resistance and it has been well established that transverse impact resistance

17

Table III

Room Temperature Charpy Impact Results for Rare Earth Modified AISI 4340 Steel

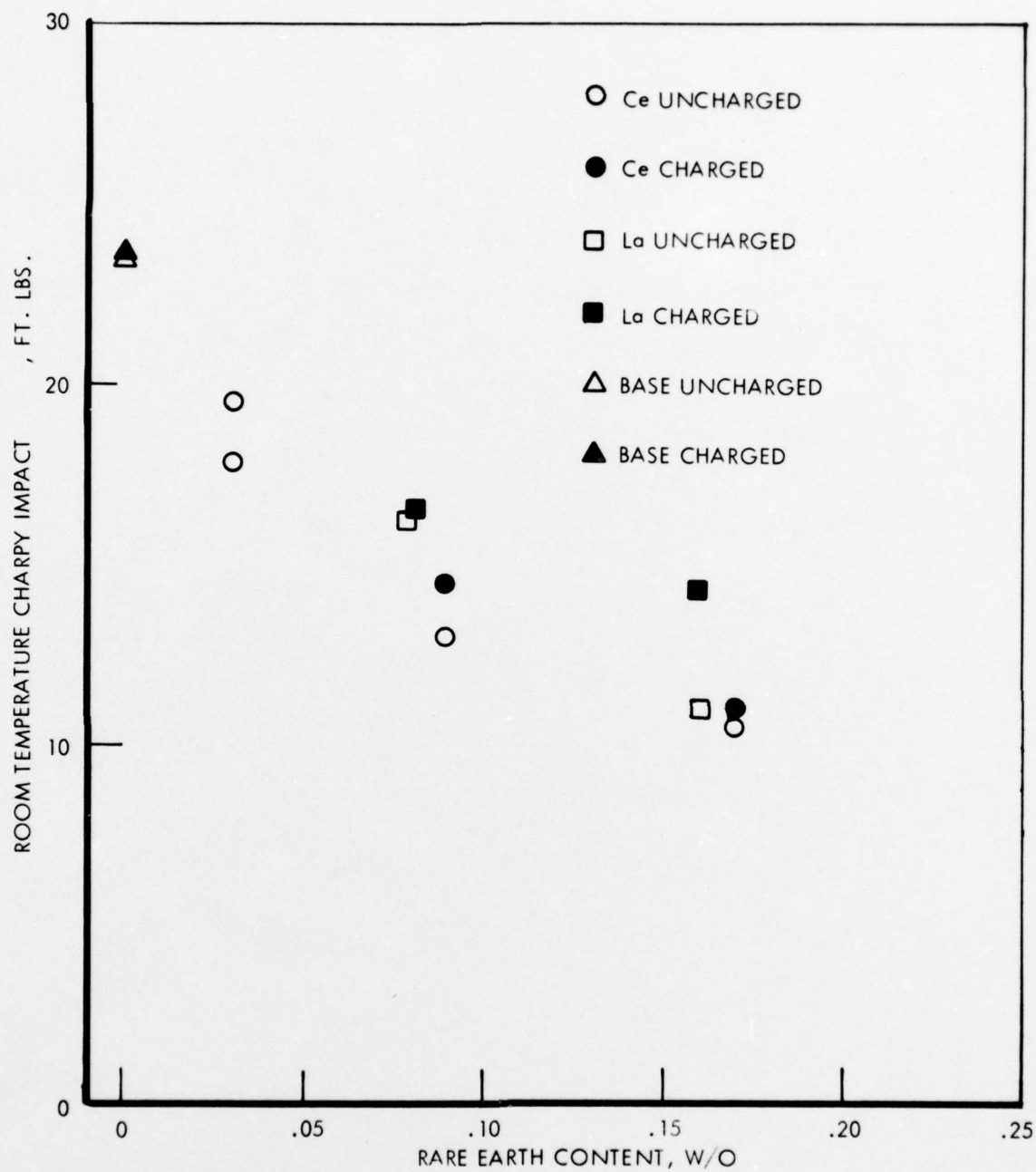| Heat	Alloy	Test Condition	Charpy Impact Load ft. lbs.
X409	Base Alloy	Uncharged	23.5
		Charged	23.5
X410	4340+0.3Ce	Uncharged	17.8
		Charged	19.5
X411	4340.09Ce	Uncharged	13.0
		Charged	14.5
X421	4340+.17Ce	Uncharged	10.5
		Charged	11.0
X412	4340+.08La	Uncharged	16.5
		Charged	16.3
X422	4340+.16La	Uncharged	11.0
		Charged	14.3

Figure 8.   Room temperature Charpy impact results plotted as a function of rare earth content in AISI 4340 steel.

reaches a maximum when the rare earth/sulfur ratio ranges from 3-4 (43,56).
For the present study, however, rare earth/sulfur ratios ranged from 8-42,
indicating that the region of optimum impact resistance had been exceeded.
Comparison of the impact results for uncharged and hydrogen charged material
indicated that charged material in general exhibited slightly improved impact
resistance, possibly because of the additional tempering effect obtained by
the 300°F (149°C) homogenization treatment given the charged material.

B.   Delayed Failure Results

        As a basis for studying the hydrogen embrittlement resistance of rare
earth modified 4340 steel delayed failure tests were conducted on specimens
cathodically charged in sulfuric acid and plated with cadmium. The results
are discussed in the following sections including failure characteristics,
crack growth behavior and metallographic evaluations.

        1.   Failure Characteristics

        Delayed failure tests, which employ a series of varying static
loads, represent a most sensitive method for studying hydrogen embrittlement.
The low strain rates allow time to develop a sufficient hydrogen concentra-
tion at the precrack to produce embrittlement. The essential characteristics
of classical delayed failure are summarized schematically in Figure 9a (57).
Note that delayed failure may occur over a wide range of applied stress and
that there is only a slight dependence of the time to failure upon the applied
stress. The most significant characteristic of delayed failure behavior,
however, is the fact that there is a minimum critical value of stress (the
lower critical stress) below which failure does not occur. Studies performed
on hydrogen-induced delayed failure of sharply notched high-strength steel
specimens indicate that an incubation time precedes crack initiation. Once
a critical amount of hydrogen has reached the area in front of the crack tip,
cracking then proceeds discontinuously until a critical length is attained,
and rapid failure occurs (53). A typical crack growth curve obtained in
delayed failure testing is shown in Figure 9b (52). The growth curves are in
reality a series of incubation periods followed by instantaneous crack
extensions (3).

        The delayed failure curves obtained in the present investigation
are presented in Figures 10-15. Note that failure times are plotted as a
function of applied stress intensity. The results indicate that rare earth
additions can have a substantial effect on failure characteristics in terms
of both failure times and lower critical stress intensity. The delayed
failure curve for the baseline 4340 material with no rare earth is shown in
Figure 10. The essential characteristics of hydrogenated high strength steels
are evident in that: (1) cracking proceeded discontinuously until a critical
length was attained followed by rapid failure, (2) failure time varied only
slightly with applied stress intensity and (3) a lower critical stress intensity
was obtained below which delayed failure was not observed after 10,000 minutes.
In this material, failures were observed within 1000 minutes at stress intensities
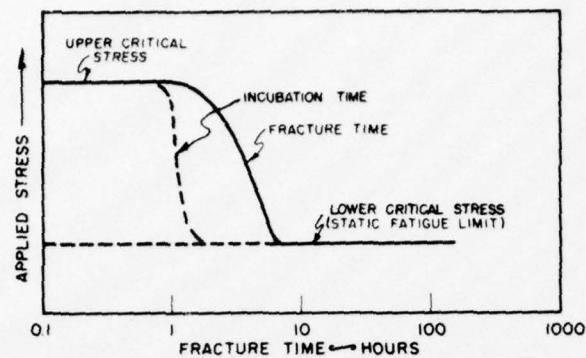
Figure 9a. Schematic representation of delayed failure characteristics of a hydrogenated high-strength steel (57).

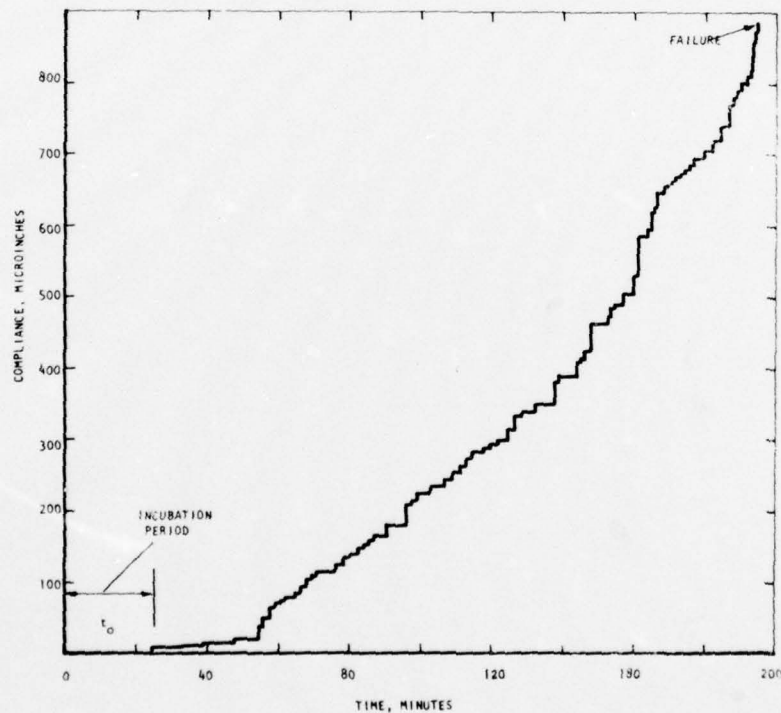Figure 9b. Typical crack growth curve for delayed failure of hydrogenated high strength steel (52).

Figure 9. Typical embrittlement characteristics for hydrogenated and plated high strength steel specimens including delayed failure and crack growth behavior.

21
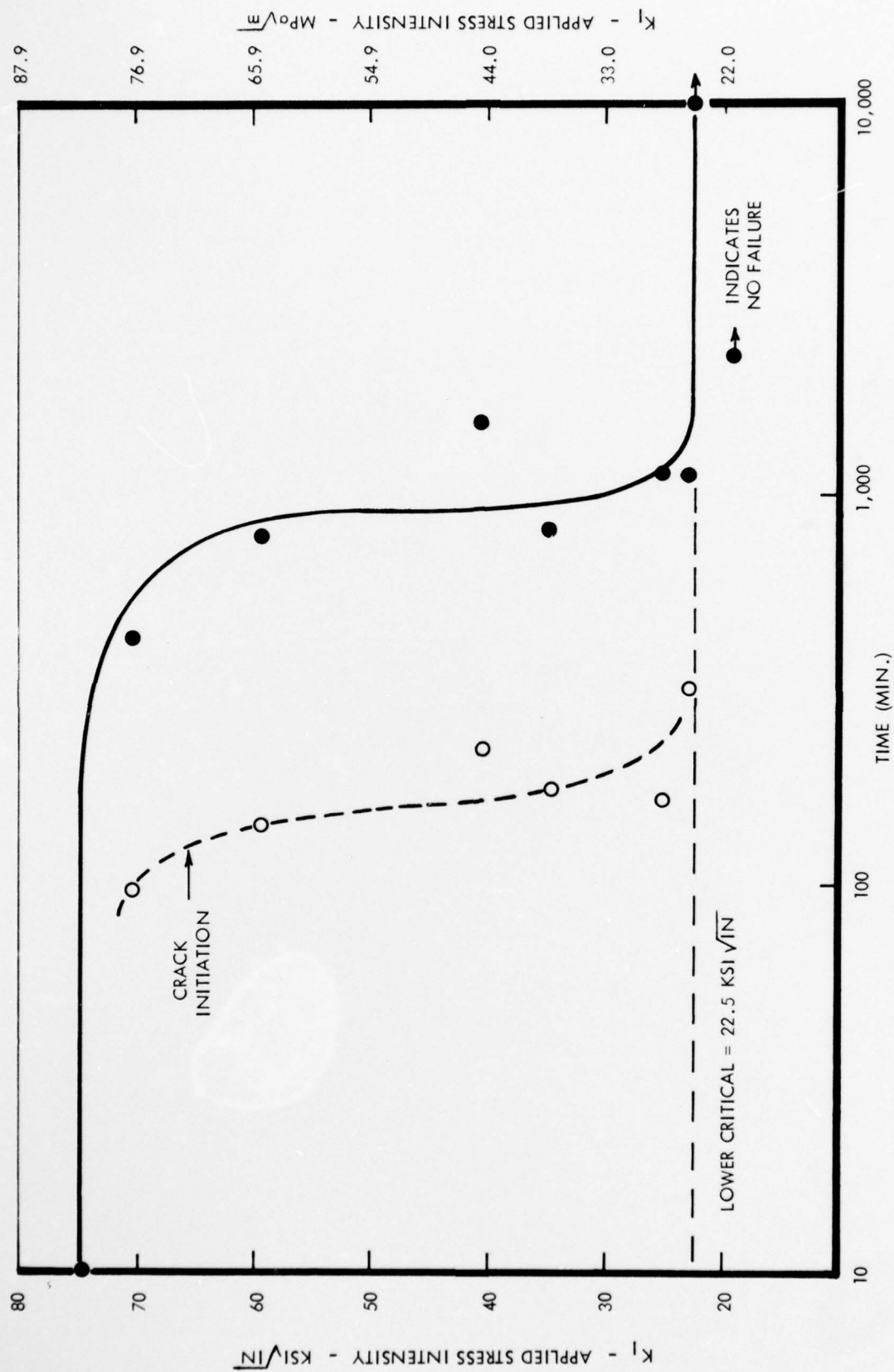
Figure 10. Delayed Failure Results for Precracked Specimens of Hydrogenated and Cadmium Plated Baseline 4340 Steel (Heat X409).

22

Figure 11. Delayed Failure Results for Precracked Specimens of Hydrogenated and Cadmium Plated 4340 Steel Plus 0.08 Weight Percent Lanthanum (Heat X412).

23

Figure 12. Delayed Failure Results for Precracked Sepcimens of Hydrogenated and Cadmium Plated 4340 Steel Plus 0.16 Weight Percent Lanthanum (Heat X422).

24

Figure 13. Delayed Failure Results for Precracked Specimens of Hydrogenated and Cadmium Plated 4340 Steel Plus 0.03 Weight Percent Cerium (Heat X410).

25

Figure 14. Delayed Failure Results for Precracked Specimens of Hydrogenated and Cadmium Plated 4340 Steel Plus 0.09 Weight Percent Cerium (Heat X411).

26
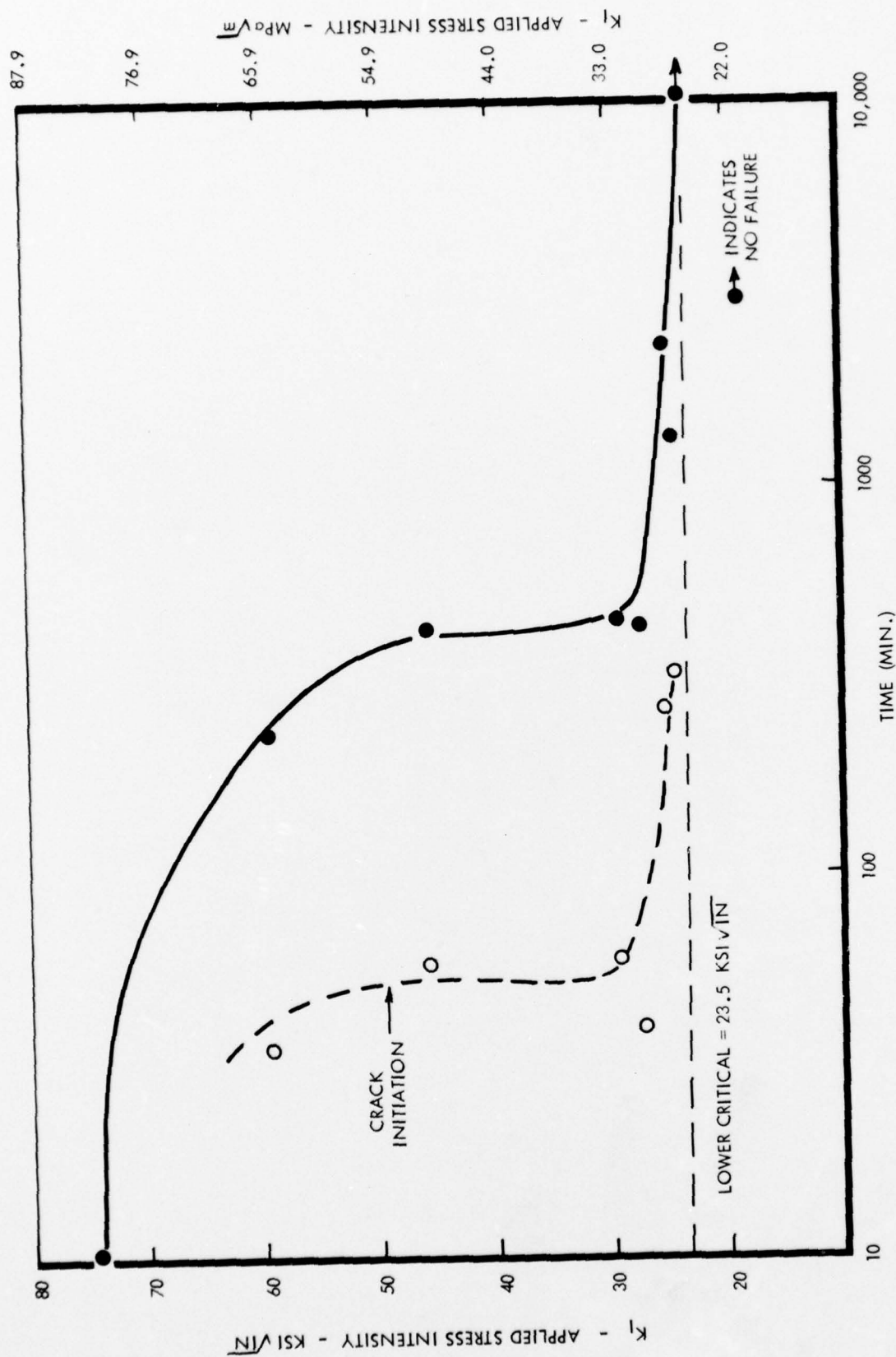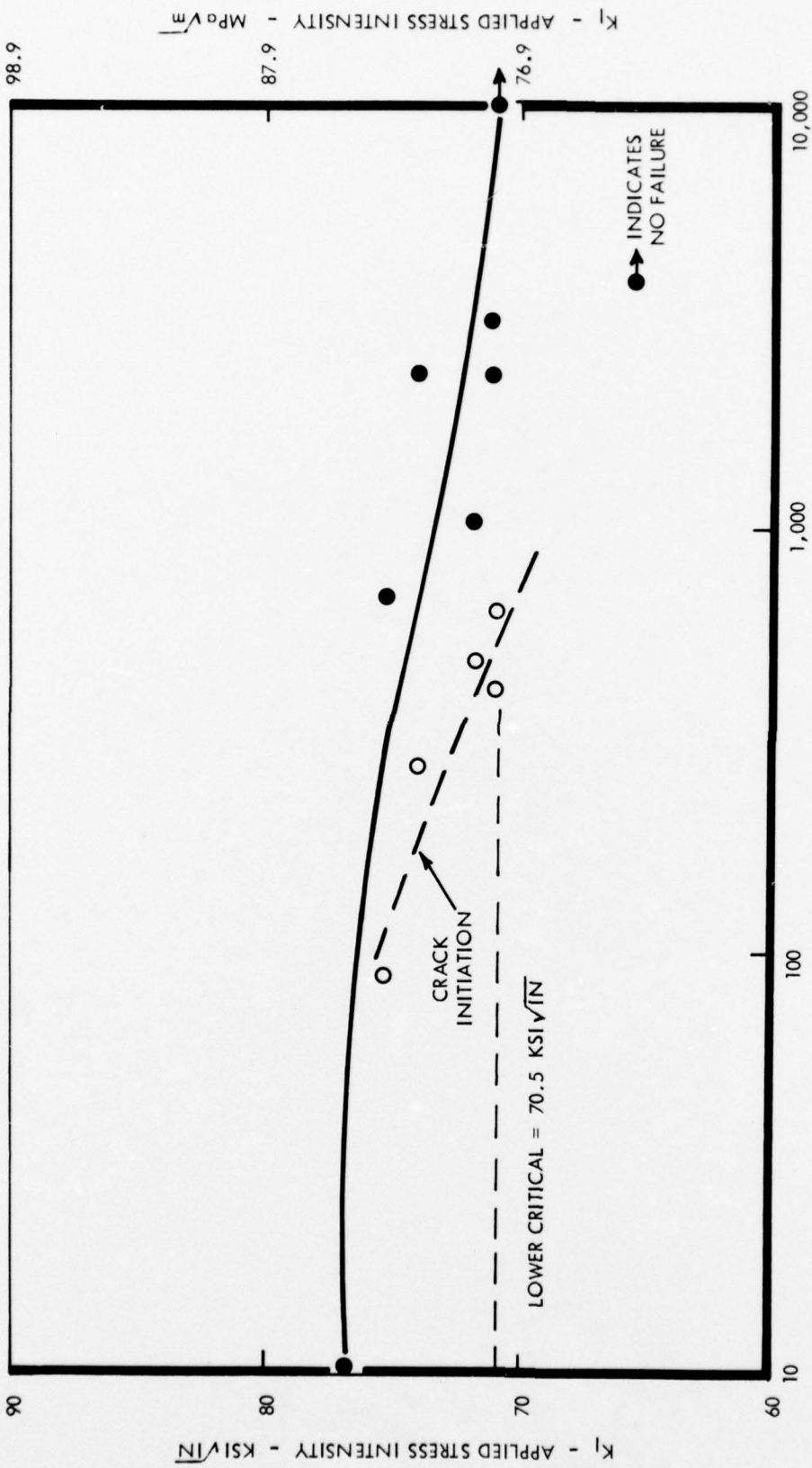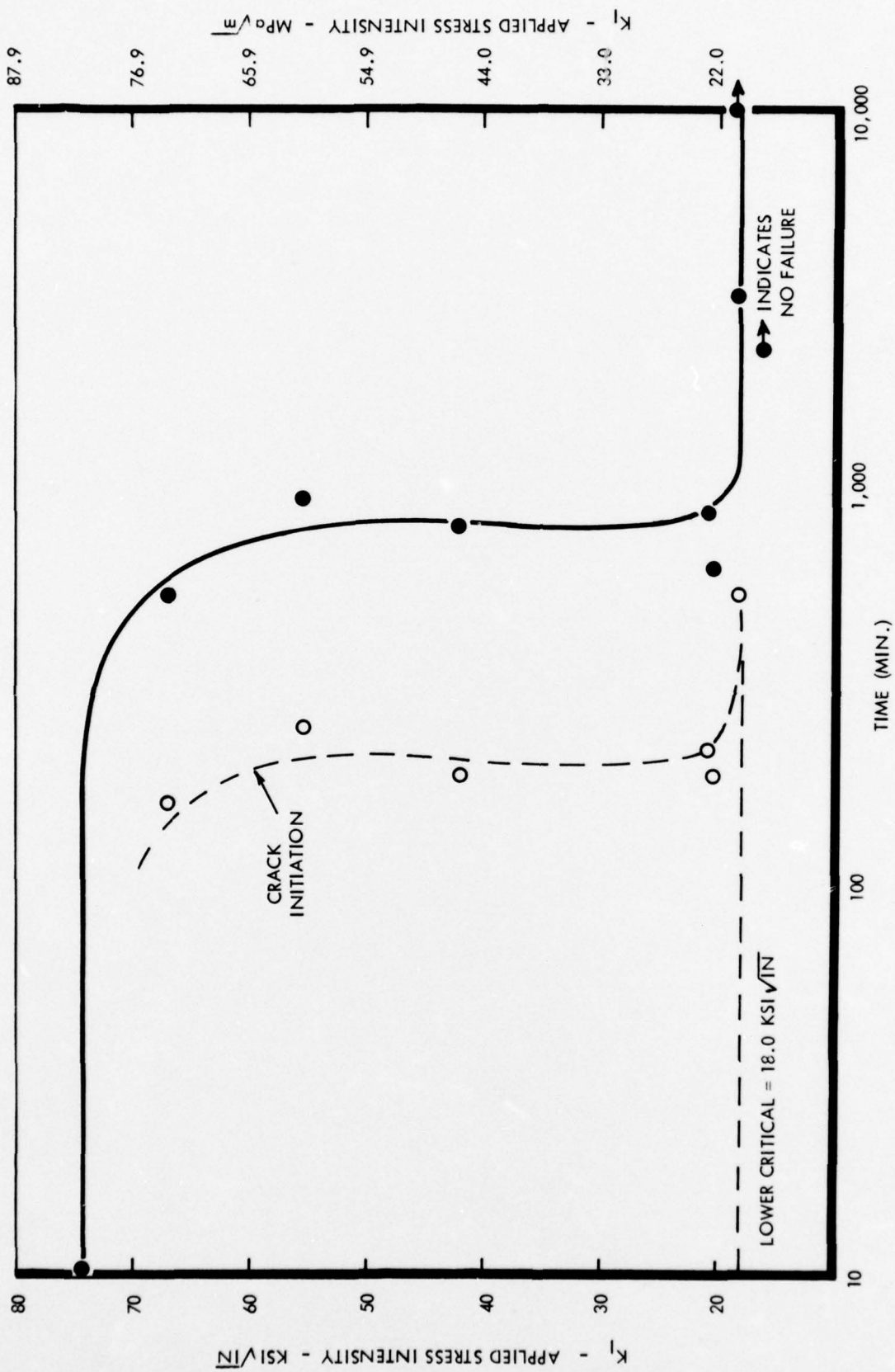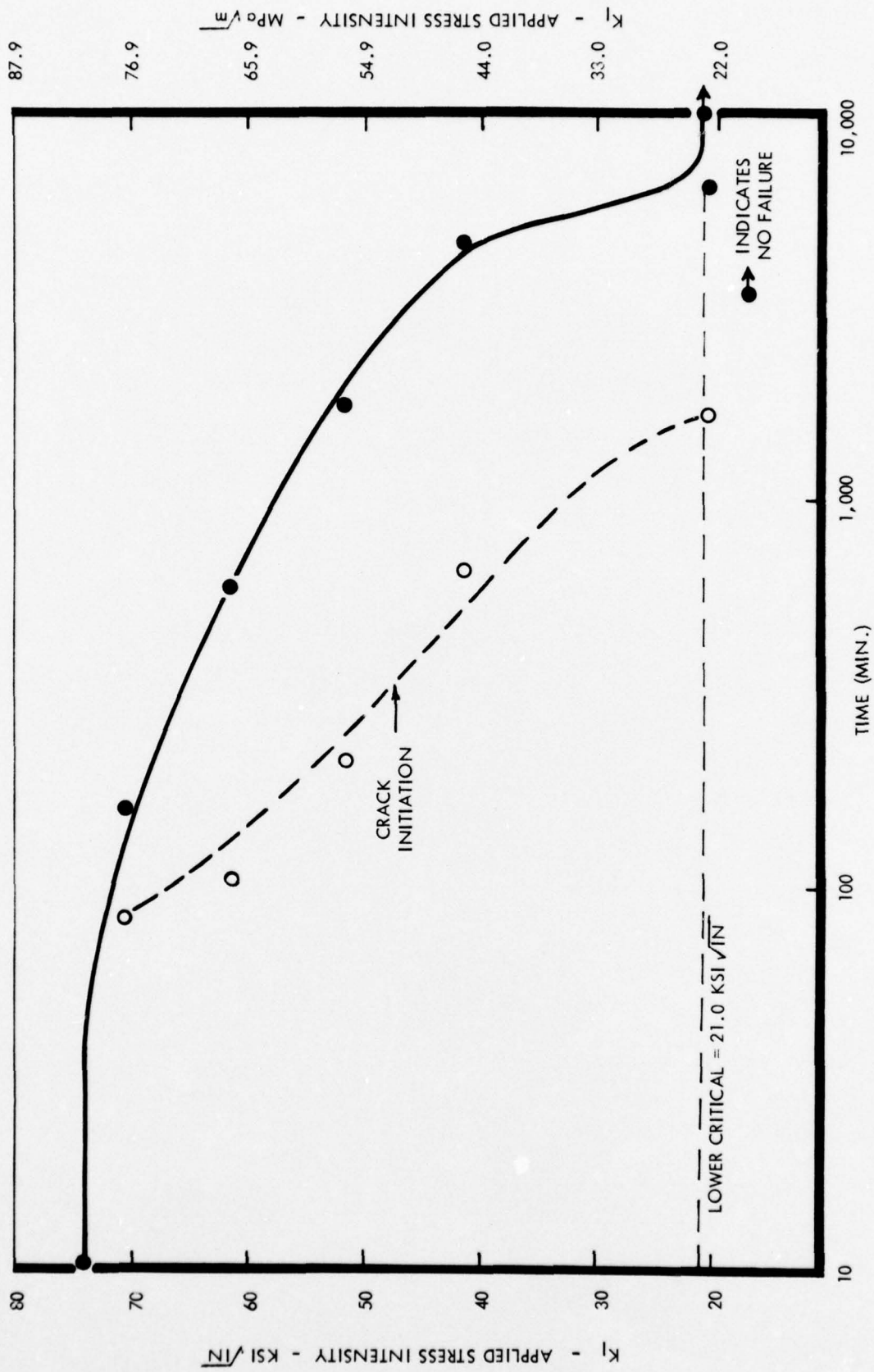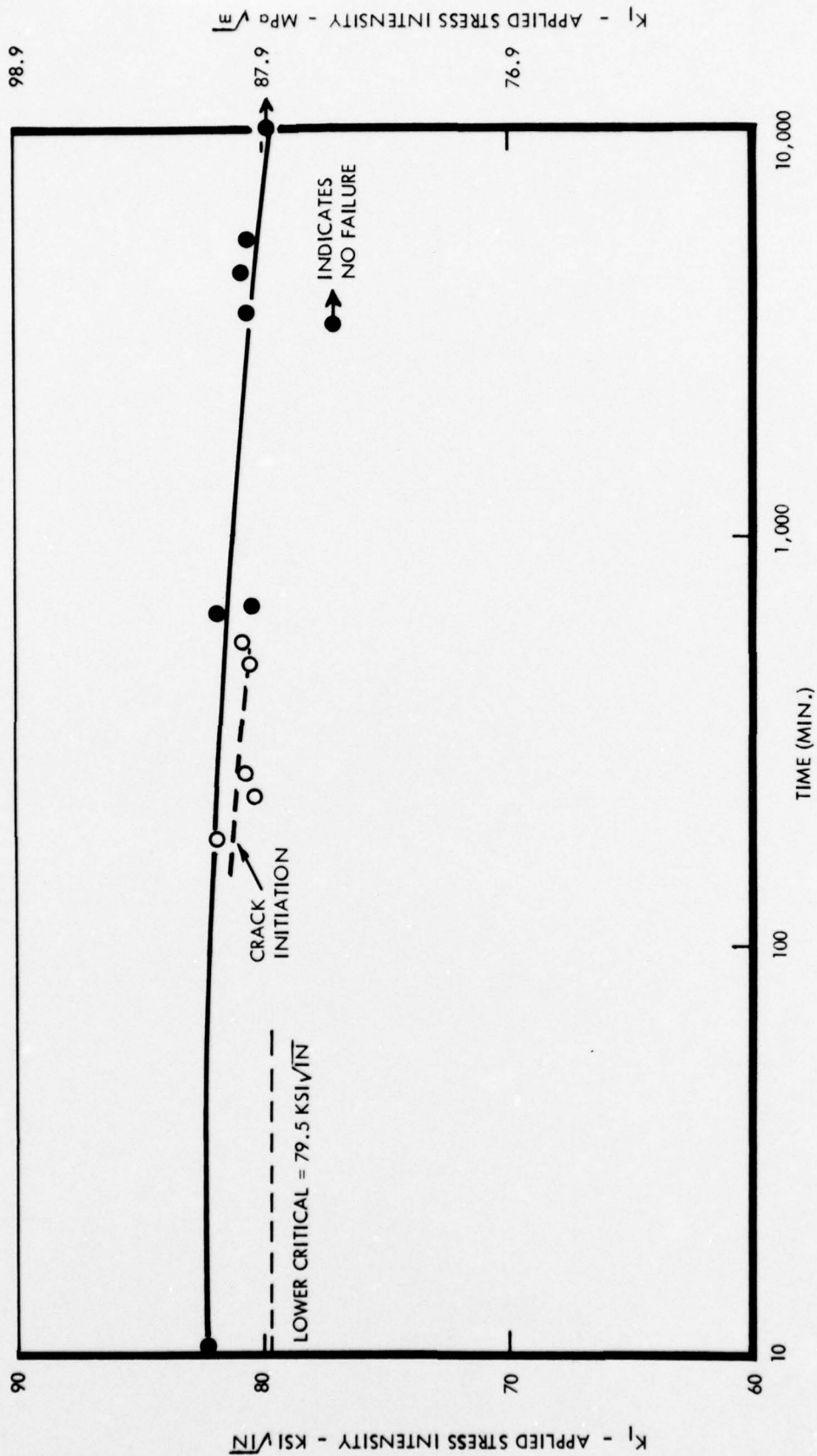
Figure 15. Delayed Failure Results for Precracked Specimens of Hydrogenated and Cadmium Plated 4340 Steel Plus 0.17 Weight Percent Cerium (Heat X421).

27

which were approximately 35-90% of the upper critical value. Crack initiation was observed at approximately 100 minutes and a lower critical stress intensity of 22.5 ksi $\sqrt{in.}$ (24.5 MPa $\sqrt{m}$) was obtained.

The effects of lanthanum additions (0.08 and 0.16 w/o levels) on delayed failure of 4340 steel are shown in Figures 11 and 12. Note the dramatic improvements both in failure times and lower critical stress intensity at the high lanthanum content. A lower critical stress intensity of 70.5 ksi $\sqrt{in.}$ (78.0 MPa $\sqrt{m}$) was obtained, representing a three-fold improvement over the non-rare earth baseline material. Crack initiation times were also much higher with the higher content lanthanum material. More important, however, was the shape of the delayed failure curve itself. The standard type curve exhibited by the baseline 4340 in Figure 10 was characterized by the rather sudden decrease from the upper critical to the lower critical stress intensity over a fairly constant range of failure times. The significance of this behavior lies in the fact that design engineers must insure that service conditions do not exceed the lower critical stress intensity. If this value is exceeded, delayed failure from hydrogen embrittlement can be expected. For the high lanthanum content material, Figure 12, the difference between the upper and lower critical values was substantially smaller than for the baseline 4340 and the decrease was much more gradual. These results suggest a significant improvement in resistance to hydrogen embrittlement compared to the baseline 4340. In particular, the high lanthanum content material can be used to a substantially higher percentage of its upper critical stress intensity without danger of delayed failure from hydrogen embrittlement. This is particularly significant for high strength steel components such as landing gears, fasteners and cables. Their production includes such operations as acid pickling cleaning and electroplating which can introduce hydrogen into the component.

The effects of cerium additions (0.03, 0.09 and 0.17 w/o levels) on delayed failure of 4340 steel are shown in Figures 13-15. In general, the results were quite similar to those for the lanthanum additions. As cerium content increased, times to crack initiation and to failure also increased. A substantial improvement in lower critical stress intensity compared to baseline 4340 was also observed with the cerium addition made at the highest level (0.17 w/o). The 79.5 ksi $\sqrt{in.}$ (87.0 MPa $\sqrt{m}$) value obtained for the cerium modified 4340 was slightly higher than the 70.5 ksi $\sqrt{in.}$ (78.0 MPa $\sqrt{m}$) value obtained with the lanthanum modified steel. These results represent approximately a 3-1/2 fold improvement over baseline 4340 and indicate that the rare earth modified steels can be designed for use to a higher percentage of their upper critical stress intensities without danger of delayed failure from hydrogen embrittlement.

The delayed failure results clearly indicated that a substantial improvement could be obtained in the hydrogen embrittlement resistance of 4340 steel through additions of cerium and lanthanum. This improvement was manifested by longer times to crack initiation (incubation time), longer failure times and higher values of lower critical stress intensity. Maximum improvement, however, was obtained only at the high rare earth levels (e.g., 0.16-0.17 w/o). As shown in Figures 5 and 6, the microstructures for these rare earth modified steels exhibited almost continuous grain boundary inclusion formations along prior austenite grain boundaries. These observations suggest a possible mechanism to rationalize the enhanced resistance to hydrogen embrittlement exhibited by the rare earth modified steel.

It is generally agreed that a critical combination of stress state and hydrogen concentration must be attained to initiate a crack (53). With a given hydrogen concentration, the lower critical stress intensity is that at which the stress state is sufficient to initiate a crack. At lower levels this critical value is not achieved and the steel is undamaged. The rationale of the incubation period, or the time required to initiate a crack, is based upon the interaction between hydrogen concentration and the stress state. Under the action of stress-induced diffusion, hydrogen migrates to the point of maximum stress triaxility, usually in close proximity to sharp defects or notches within a component. When the hydrogen concentration attains a critical value (constant for a given applied stress) a crack initiates at this location and delayed failure ensues. If the transport of hydrogen can be interrupted or delayed, then an extended time interval would be necessary to build up the hydrogen at the point of crack initiation.

The results of the present investigation suggest that the ability of rare earth elements to getter or otherwise entrap hydrogen was responsible for the improved resistance to hydrogen embrittlement. That maximum improvement was obtained only at the higher rare earth levels can be rationalized by the fact that larger amounts of cerium and lanthanum were required to effectively delay the critical value of hydrogen concentration from being reached at the crack tip. Effective hydrogen entrappment also resulted in a much higher magnitude of stress state being required to propagate the precrack. Under an alternative set of charging conditions different amounts of hydrogen would be introduced into the component, resulting in the fact that changes in rare earth content would be required to obtain similar inhibitive results. At the lower rare earth levels used in the present study it was apparent that the critical hydrogen concentration was achieved in spite of the fact that certain amounts were probably entrapped enroute to the crack tip. It can thus be appreciated how a microstructure consisting of continuous grain boundary rare earth inclusions would represent a highly effective barrier against hydrogen diffusion throughout a high strength steel component.

2. Crack Growth Behavior

The principal characteristic of sub-critical crack growth under hydrogen embrittlement conditions is that the rate of crack propagation, da/dt, is primarily a function of K_I, the stress intensity factor at the crack tip. Under steady state conditions of crack growth, K_I is thus taken to be a proper representation of the mechanical crack driving force (58). Typical steady state crack growth response as a function of K_I is shown schematically in Figure 16. The relation of K_I to the logarithm of crack growth rate can be separated into three distinct regions. Region I is highly dependent on K_I, and may reflect crack acceleration for certain types of tests. K_{th} is the stress intensity factor at which cracking begins in times of engineering significance (related to the particular application of engineering structure). Region II is nearly independent of K_I and represents a range where crack growth is probably limited by the rate of the hydrogen diffusion process. In Region III, crack growth approaches the condition for unstable growth because of overload. For high strength materials, under conditions approximating plane strain, the condition for the onset of unstable growth is defined by $K_I = K_{Ic}$, where K_{Ic} is the plane strain fracture toughness of the material.

In the present investigation crack growth kinetics were measured with the use of compliance gages which recorded crack opening displacements during each of the delayed failure tests. Calibration specimens were utilized to determine the relationships between crack opening and crack length. The results of these studies are shown in Figure 17 and indicate that the individual crack growth rate curves were grouped into two distinctly separate bands of data. In the band to the lower right were included all the crack growth curves for the 4340 steel modified with rare earths at the high levels (i.e., 0.16-0.17 w/o). In the band to the upper left were included all the crack growth curves for the baseline 4340 as well as the rare earth modified steels at the lower rare earth contents. Comparison with the schematic representation of crack growth kinetics under sustained loads shown in Figure 16 indicates that the data bands obtained in the present study are representative of the transition zone from Regions I to II, where crack growth rate is nearly independent of K_I and unstable fracture has not yet occurred. That the crack growth data could be represented by such bands reflected the fact that within each band there were no definite trends available to establish significant differences between the various heats of steel. This variability or scatter between individual crack growth curves has been observed previously especially in stress corrosion testing (58). In particular, incubation time variability, nonsteady-state crack growth and the magnitude of initial K_I have all been shown to exert a considerable influence upon sustained load crack growth kinetics.
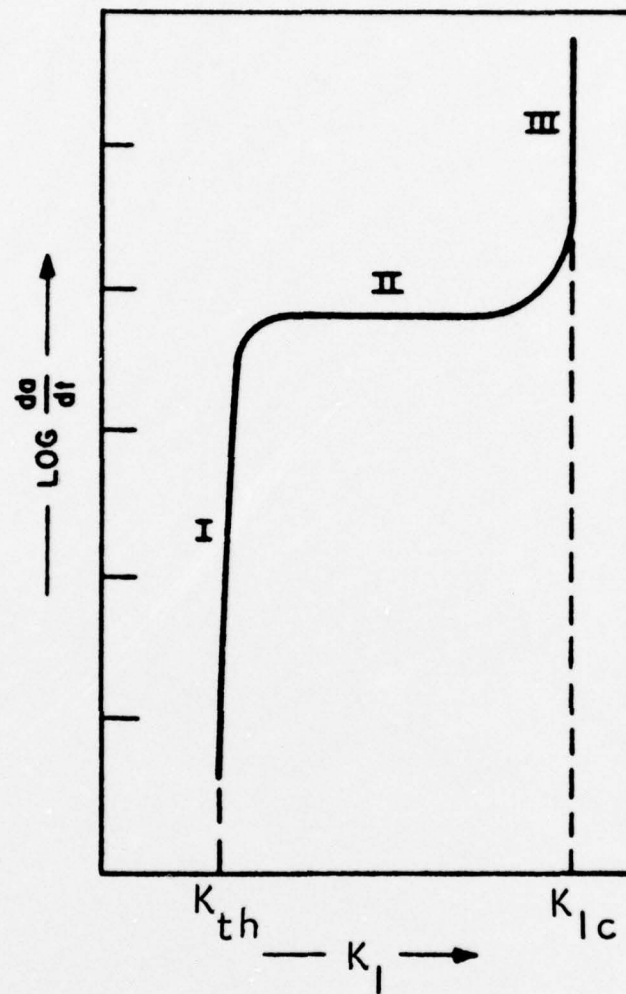
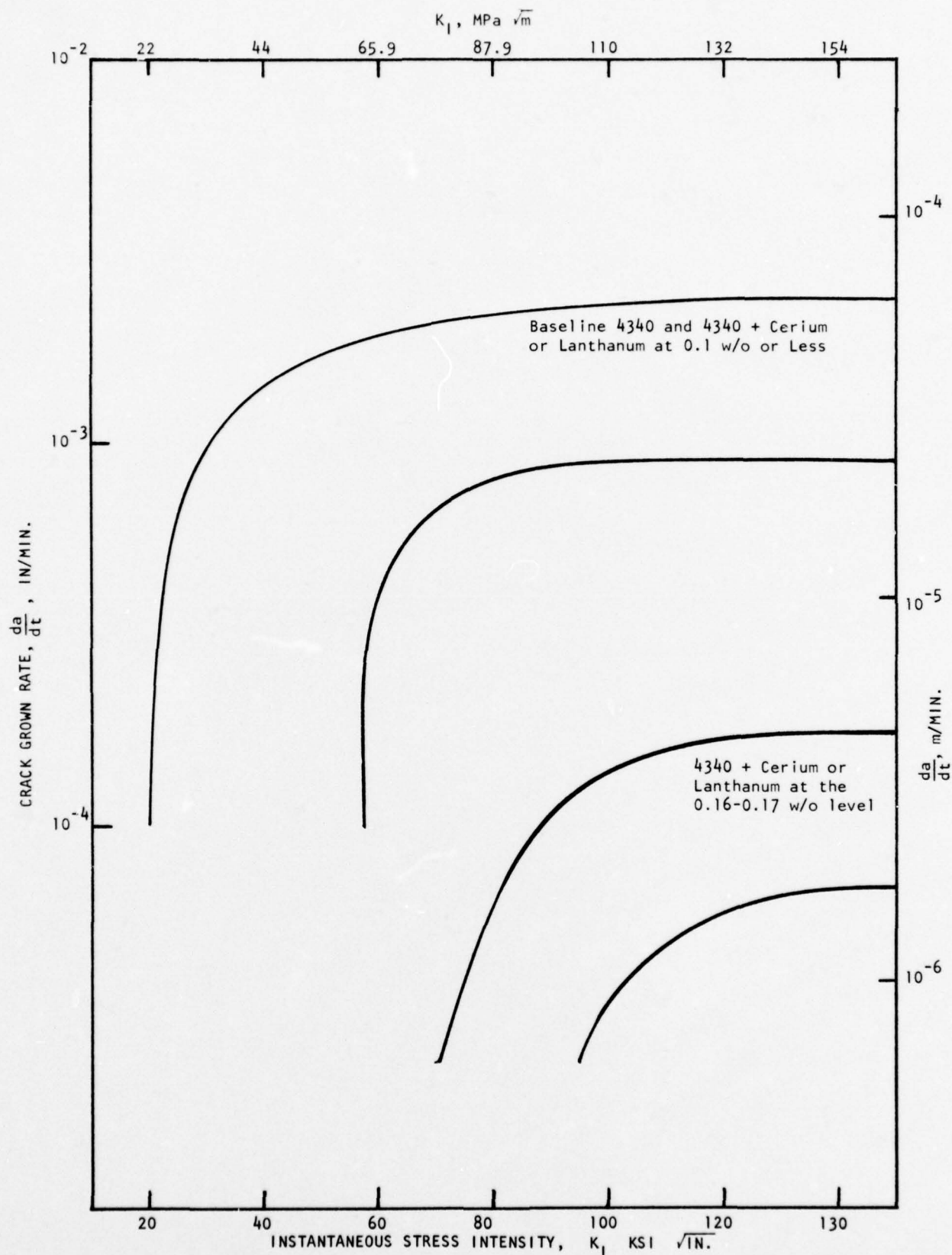Figure 16. Schematic Representation of Crack Growth Kinetics Under Sustained Load (58).

Figure 17. Delayed Failure Crack Growth Rate Results for Precracked Specimens of Hydrogenated and Cadmium Plated Baseline 4340 Steel and Rare Earth Modified 4340 Steel.

In spite of the fact that significant trends could not be established between the heats of steel in the various bands, the differences between the bands themselves were significant. In the high rare earth steels, for example, crack growth was not observed until the initial applied stress intensity had exceeded 70 ksi $\sqrt{in.}$ (76.9 MPa $\sqrt{m}$). In the baseline 4340 and low rare earth level steels, however, crack growth at this stress intensity level was already approaching the Region II plateau. At comparable stress intensity levels, ranging from approximately 100 ksi $\sqrt{in.}$ (110 MPa $\sqrt{m}$) to 130 ksi $\sqrt{in.}$ (143 MPa $\sqrt{m}$), crack growth kinetics in the baseline 4340 and low rare earth steels was an order of magnitude faster than that exhibited by the high rare earth steels. As a first approximation these results indicate that the safe operating life for high rare earth steel components would be considerably greater than for the baseline or low rare earth steels. This crack growth behavior can be explained on the basis of hydrogen diffusing to the crack tip and resulting in discontinuous crack growth. In the high rare earth content material, the continuous grain boundary inclusions acted to entrap hydrogen, inhibiting its transport to the crack tip. Crack propagation was subsequently retarded. In the baseline material and the low rare earth steel, the transport of hydrogen was not seriously interferred with and crack propagation was not retarded.

3.   Metallographic Evaluation

Metallographic evaluations including light and scanning electron microscopy and electron microprobe analyses were conducted on selected specimens to aid in the interpretation of the delayed failure results. The metallographic analyses indicated two distinctly different types of characteristics grouped much along the same lines as the crack growth results. The baseline 4340 steel and that modified with rare earths at the low levels (<0.1 w/o) exhibited one type of behavior while that modified with rare earths at the high levels (>0.15 w/o) exhibited another type of behavior. In general, the fracture surfaces of specimens representing baseline 4340 behavior contained a duplex type appearance. Starting near the fatigue precrack was an extensive area of predominantly intergranular fracture morphology. As the hydrogen induced crack growth proceeded in the specimens, the amount of intergranular morphology decreased, being replaced by a dimple rupture morphology. At the point of unstable crack growth due to overload, the fracture appearance was completely dimple rupture in nature. This basic fracture appearance was the same regardless of the value of initial applied stress intensity. However, specimens tested at higher initial stress intensity levels exhibited much smaller regions of intergranular fracture morphology. This suggested that much less hydrogen induced crack growth occurred before the stress intensity levels required to cause overload failures were reached.

As shown by the scanning electron microphotographs in Figures 18 and 19, the fracture appearances of 4340 steel modified with rare earths at the high levels were substantially different from those characterized by the baseline 4340 steel. The photos in these figures were taken at 500X magnification at a point approximately 0.04" (5 mm) away from the fatigue precrack.
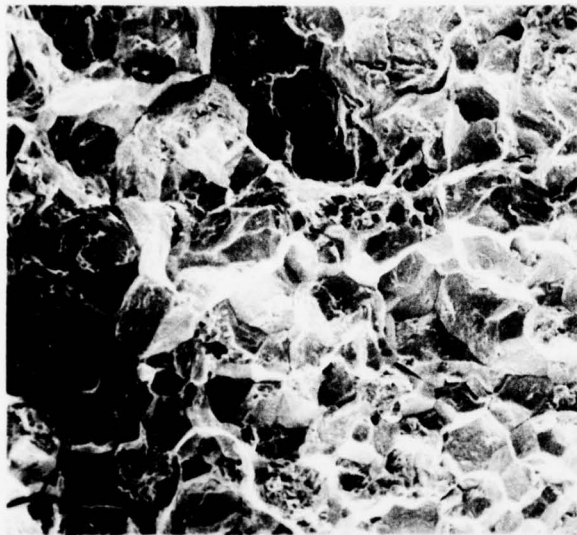
a) Heat X409 - No Rare Earth Addition
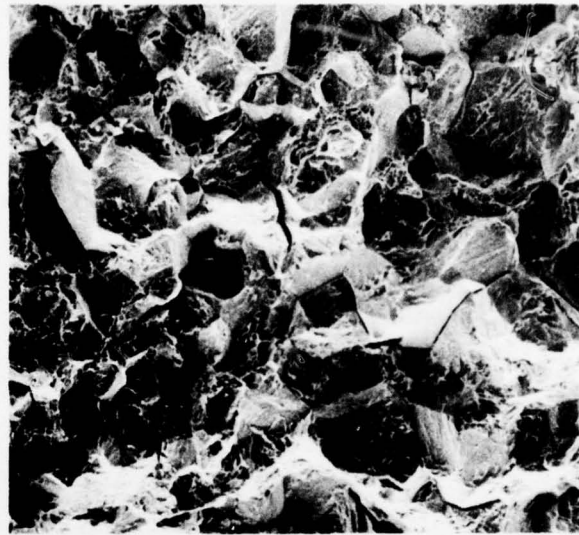
b) Heat X410 - 0.33 w/o Cerium

c) Heat X411 - .092 w/o Cerium
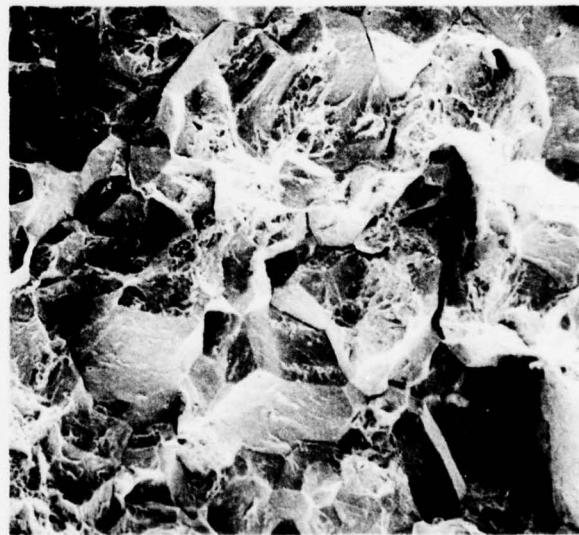
d) Heat X412 - .078 w/o Lanthanum

Figure 18. Scanning Electron Microphotographs Taken at 500X. Magnification of the Fracture Surfaces of 4340 Baseline Steel and 4340 Steel Modified with Rare Earths at the Low Levels (<0.1 w/o). Photos Were Taken at a Point 0.04" (5 mm) From Fatigue Precrack.

a) Heat X421 - 0.17 w/o Cerium
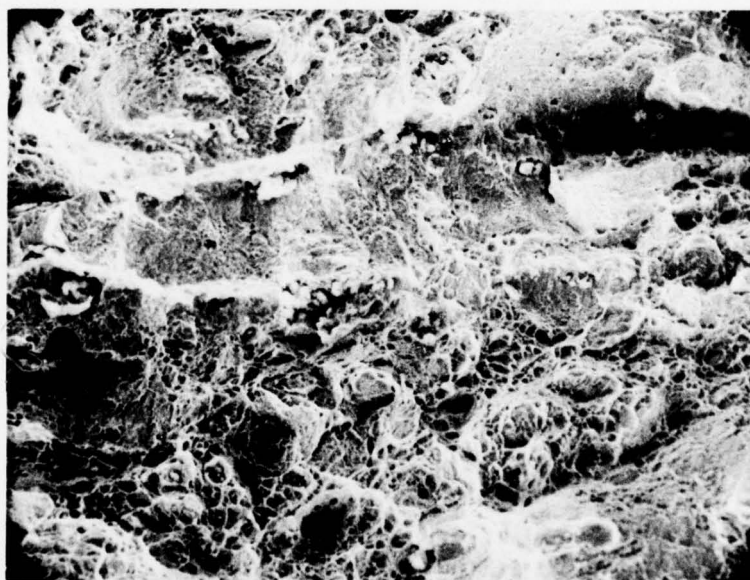
b) Heat X422 - 0.16 w/o Lanthanum

Figure 19. Scanning Electron Microphotographs Taken at 500X.
Magnification of the Fracture Surfaces of 4340
Steel Modified with Rare Earths at the High Level
(>0.15 w/o). Photos were Taken at a Point 0.04"
(5 mm) From Precrack.

35

The intergranular fracture morphology shown in Figure 18 for the baseline 4340 type behavior was indicative of hydrogen induced crack growth. Note the appearance of greater amounts of intergranular material (rare earth oxide inclusions) on the fracture surface as rare earth content increases. In contrast to this, the fracture surfaces shown in Figure 19 for the high rare earth content material are primarily dimple rupture in appearance. This overload type of fracture morphology was characteristic of the entire fracture surface of these specimens. It must be pointed out that crack growth was not observed in these materials until much higher levels of stress intensity were attained compared to the baseline type material. Thus, little hydrogen assisted crack growth occurred in these specimens before the onset of unstable crack growth and overload failure.

IV SUMMARY AND CONCLUSIONS

Experiments were conducted to develop a method to inhibit the effect of hydrogen embrittlement in high strength steels. The investigation included a study of the effect of cerium and lanthanum rare earth additions made to AISI 4340 steel in an effort to getter or entrap hydrogen. The experimental approach involved first a determination of the influence of various amounts of these rare earths on the baseline mechanical properties of 450°F (230°C) temper material including room temperature tensile and Charpy impact tests. Resistance to hydrogen embrittlement was then characterized in terms of delayed failure tests conducted on specimens cathodically charged in sulfuric acid and plated with cadmium. The results were analyzed to determine which element had the greatest potential to improve the hydrogen embrittlement resistance of 4340 steel.

For this investigation lanthanum and cerium were added at the 0.1-0.2 weight percent (w/o) levels to aluminum deoxidized vacuum induction melted ingots. Forging and cross rolling were conducted utilizing breakdown procedures representative of typical operations conducted within the steel making industry. The ability to work this ingot to plate form clearly demonstrated the workability of 4340 steel made with the level of rare earth additions studied in this program.

Room temperature tensile results for both uncharged and hydrogen charged material were comparable and indicated little difference between the elements. A maximum occurred in the ultimate and 0.2% yield strengths at approximately 0.1 w/o for both rare earth additions. This strengthening behavior was attributed to the deoxidizing and desulfurizing action of the rare earths. At higher rare earth contents, massive and continuous rare earth oxide inclusions formed at prior austenite grain boundaries resulting in a slight (4%) decrease in strength properties compared to the baseline material.

The room temperature percent elongation, percent reduction of area and Charpy impact energy all decreased with the addition of both cerium and lanthanum. Again, there was little difference between the elements or between charged and uncharged material. In spite of this ductility loss, however, only the lanthanum modified 4340 would not have met the required ductility specifications for Aircraft Quality 4340 in this temper (transverse percent elongation - 6% minimum, transverse percent reduction of area - 25% minimum). At the high rare earth levels the Charpy impact energies decreased to approximately 15% below 13.0 ft. lb. Aircraft Quality specification. The ductility and impact losses in these steels were attributed to the formation of massive and continuous grain boundary inclusions which offered ideal paths for crack propagation.

The delayed failure results indicated that a substantial improvement could be obtained in the hydrogen embrittlement resistance of 4340 steel through additions of cerium and lanthanum. Improvement could be observed in terms of longer times to crack initiation (incubation time), longer failure times, higher values of lower critical stress intensity and lower crack growth rates compared to baseline 4340 material. It is important to note, however, that the maximum improvement was obtained only at the high rare earth levels (e.g., 0.16-0.17 w/o) for both elements. The most significant aspects of this increased resistance to hydrogen embrittlement were manifested in terms of higher values of lower critical stress intensity and lower crack growth rates. For example, the lower critical stress intensities for the high content rare earth steels were approximately three times higher than that of the 4340 base-line material. Cerium, with a value of 79.5 ksi $\sqrt{in.}$ (87.0 MPa $\sqrt{m}$) was slightly more beneficial than lanthanum, 70.5 ksi $\sqrt{in.}$ (78.0 MPa $\sqrt{m}$), in this respect. These considerations suggest that the high rare earth content steels can be designed for use to a higher percentage of their upper critical stress intensities without danger of delayed failure from hydrogen embrittlement. The crack growth results were included in a band of data indicating there were no significant differences between the lanthanum or cerium additions. However, comparison with the baseline 4340 and low rare earth steels indicated that crack growth was an order of magnitude lower in the high rare earth steels. As a first approximation these results indicate that the safe operating life for high rare earth steel components would be considerably greater than for the baseline or low rare earth steels.

The results of this study suggest that the ability of rare earth elements to getter or otherwise entrap hydrogen was responsible for the improved re-sistance to hydrogen embrittlement. That improvement was obtained only at the high rare earth levels was rationalized on the basis of the fact that larger amounts of cerium and lanthanum were required to effectively delay the critical value of hydrogen concentration from being reached at the crack tip. Effective hydrogen entrapment also resulted in a much higher magnitude of stress state being required to propagate cracks.

V RECOMMENDATIONS FOR FUTURE WORK

In this study it was demonstrated that a significant improvement can be obtained in the hydrogen embrittlement resistance of hydrogenated and plated AISI 4340 steel. Additions of lanthanum and cerium at approximately 0.15 weight percent resulted in substantial improvement in hydrogen embrittlement resistance including increased times to crack initiation and failure, higher values of lower critical stress intensity and significantly lower crack growth rates. Further work is required, however, before the technical approach and inhibition methods developed in this study can be applied to a wider range of hydrogen embrittlement problems.

For example, additional studies should be initiated to improve the baseline mechanical properties of the rare earth steels. The rare earth levels characterized by the most significant improvements in resistance to hydrogen embrittlement resulted in microstructures containing continuous grain boundary rare earth oxide inclusions. These were ideal fracture paths and resulted in a decrease in room temperature ductility and Charpy impact energy. Efforts should be concentrated on melting techniques to minimize the formation of these film-like inclusions. An alternative approach might be optimized forging and/or ingot breakdown procedures incorporating controlled amounts of deformation to homogenize this microstructure.

Another important area of future research should be the development of a more basic understanding of the mechanisms responsible for this inhibition behavior. Studies here should include permeability measurements and the hydrogen analysis of specimens hydrogenated at various charging conditions. If the large differences in the kinetics and failure times of the hydrogenated 4340 steel of different rare earth content are due to the differences in hydrogen mobility or the fact that hydrogen is being trapped, then permeability measurements using the time lag to obtain a measure of apparent hydrogen diffusivity should show a difference which can be directly correlated with delayed failure. Hydrogen analyses would also be useful for substantiating the ability of rare earths to getter hydrogen. Once failure has occurred in the hydrogenated and plated specimens, the uncombined hydrogen can diffuse through the matrix and exit through the fresh fracture surface. If hydrogen has been trapped by the rare earth getters, however, it cannot diffuse and remains instead in its combined form within the specimen. Thus, specimens with higher rare earth contents should contain larger amounts of entrapped hydrogen.

Finally, the trend of the rare earth effects characterized in the present program indicated that the inhibition behavior was extremely sensitive to rare earth content. This critical rare earth content may vary with alloy system and with the type of hydrogen embrittlement problem anticipated in service. Once an understanding of the basic mechanisms responsible for rare earth inhibition has been achieved, this approach can be expanded to other type high strength steels and service environments or conditions. It is anticipated that such studies would include efforts to optimize the rare earth content for the particular alloy or application.

VI REFERENCES

1. J. D. Fast, "Interaction of Metals and Gases, Academic Press, New York, 1965.

2. P. Cotterill, "The Hydrogen Embrittlement of Metals," Prog. Mat. Sci., 9(4):205, 1961.

3. E. A. Steigerwald, F. W. Schaller, and A. R. Troiano, Transactions, Metallurgical Society of AIME, Vol. 215, December 1959, pp. 1048-1052.

4. A. R. Troiano, Metal Progress, Vol. 77, February pp. 112-117.

5. M. Smialowsky, Hydrogen in Steel, Addison-Wesley, Reading, Mass., 1962.

6. A. E. Schuetz and W. D. Robertson, Corrosion, Vol. 13, July 1957, pp. 437t-458t.

7. E. Folkhard, H. Schabereiter, G. Rabensteiner, and H. Tettenbacher, L'Hydrogene dans les Metaux, 501, 1972.

8. L. A. Glikman and V. A. Orlov, Soc. Mat. Sci., 4(1):106, 1968.

9. V. N. Kudryavtsev, K. S. Pedan, N. K. Baraboshkina, and A. T. Vagramyan, L'Hydrogene dans les Metaux, 253, 1972.

10. J. P. Fidelle, J. Legrand, and C. Couderc, TMS Paper No. F71-8 of Met. Soc. of AIME, New York.

11. M. Smialowski, Hydrogen in Steel, Addison-Wesley, Reading, Mass., 1962.

12. A. A. Sheinker and J. D. Wood, Stress Corrosion Cracking of Metals, Chapter 2, ASTM STP 518, October 1971, pp. 16-39.

13. R. N. Parkins, Met. Reviews, Vol. 9, No. 35, 1964, pp. 201-260.

14. W. Hofmann and W. Rauls, Arch. Eisenhuttenswesen, Vol. 32, March 1961, pp. 169-173.

15. R. P. Gangloff, "Gaseous Hydrogen Embrittlement of High Strength Steel," Ph.D. Thesis, Lehigh University, 1974.

16. J. H. Schwartz and J. J. Ward, "Direct Energy Conversion," NASA SP-5057 National Aeronautics and Space Administration, Washington, D.C., 1968.

17. W. E. Moeckel, "Propulsion Systems for Manned Exploration of the Solar System," NASA TM X-1864, National Aeronautics and Space Administration, Washington, D.C., 1969.

18. B. Syrett, "Materials Requirements in a Hydrogen Economy-New Challenges," Presented at TriService Corrosion of Military Equipment Conference, 29-31, October 1974, Dayton, Ohio.

19. R. Lagneborg, "Hydrogen Embrittlement in Austenitic Steels and Nickel Base Alloys," J. IRSI, 207 (3), 1969, pp. 363-366.

20. W. Beck et al, "Hydrogen Stress Cracking of High Strength Steels," Naval Air Development Center Report NADC-MA-7140, December 23, 1971, p. 195.

21. I. M. Bernstein, "Alloy Design to Resist Hydrogen Embrittlement," Presented at MATCON 74 Conference and Materials Science Symposium, October 1974, Detroit, Michigan.

22. G. Scahs and W. Beck, "Survey of Low Alloy Aircraft Steels, Heat Treated to High Strength Levels," Pt. 1 Hydrogen Embrittlement WADC Technical Report, 53/254, Air Force Materials Laboratory (WPAFB) Dayton, Ohio, 1954.

23. C. E. Sims, G. A. Moore and D. W. Williams, "The Effect of Hydrogen on the Ductility of Cast Steels," Trans. AIME, 176, 1949, pp. 283-308.

24. A. R. Troiano, "Delayed Failure of High Strength Steel," Corrosion, 15, 1959, pp. 207t-212t.

25. R. D. Johnson, J. H. Johnson, J. G. Morlet and A. R. Troiano, "Effects of Physical Variables on Delayed Failure in Steel," WADC Technical Report 57-220, Air Force Materials Laboratory (WPAFB) Dayton, Ohio, 1956.

26. J. F. Bates, "Thermomechanical Effects on Stress Corrosion Cracking of Austenitic Stainless Steels," Mater, Protection, 9, 1970, pp. 27-32.

27. C. S. Carter, "Effect of Prestressing on the Stress-Corrosion Resistance of Two High-Strength Steels," Met. Trans., Vol. 3, February 1972, pp. 584-586.

28. C. A. Zapffe and M. E. Haslem, "Hydrogen Embrittlement in Cadmium and Zinc Electroplating," Plating, 37 (4), 1950, pp. 366-371.

29. F. S. Williams, W. Beck and E. J. Jankowsky, "A Notched Ring Specimen for Hydrogen Embrittlement Studies," Proc. ASTM, 60, 1960, pp. 1192-1202.

30. W. Beck and E. J. Jankowsky, "The Effectiveness of Metallic Undercoats in Minimizing Plating Embrittlement of Ultra High Strength Steel," Proc. Am Electroplaters' Society, 47, 1960, pp. 152-159.

31. "Investigation of Hydrogen Embrittlement of Silver Plated 4340 Steel at Various Strength Levels," Report 9080, Ser, No. 20, McDonnel Aircraft Corp., St. Louis, Mo., February 1962.

32. H. H. Uhlig, Corrosion and Corrosion Control, John Wiley & Sons, New York, 1963, p. 182.

33. L. J. McEowan and A. R. Elsea, "Behavior of High Strength Steels Under Cathodic Protection," Corrosion, 21, 1965, pp. 28-37.

34. F. N. Speller, Corrosion, Causes and Prevention, 3rd Edition, McGraw-Hill, New York, 1951, pp. 320-376.

35. G. E. F. Brewer, "Actively Corrosion Resistant Coatings?", Metal Finishing, August 1974, pp. 49-50.

36. R. P. Wei and G. W. Simmons, "Environment Enhanced Fatigue Crack Growth in High-Strength Steels," Technical Report No. 1, Contract N00014-67-A-0370-0008, NR 036-097, March 1973.

37. H. W. Liu, Ya-lung Hu and P. J. Ficalora, "Catalytic Dissociation and Hydrogen-Assisted Cracking," Paper Presented at 1973 Western Metal and Tool Conference, March 12, 1973.

38. H. R. Baker and C. R. Singleterry, "The Effect of Some Electrolytes on the Stress Corrosion Cracking of AISI 4340 Steel," Corrosion, Vol. 28, No. 9, September 1972.

39. D. C. Zecher, "Corrosion Inhibition by Surface-Active Chelants," Materials Performance, April 1976, pp. 33-37.

40. I. G. Davies, M. Randle and R. Widdowson, "Distribution of Inclusions in Rare Earth Treated Steel Ingots," Metals Technology, May 1974.

41. P. G. Barnard, "Effects of Rare Earth Additions on Plain-Carbon Steel," U.S. Bureau of Mines, Rept. Invest. No. 6907, 1967.

42. "Nonmetallic Inclusions in Continuously Cast Low Alloy Steel Treated with Rare Earths," Report to Molybdenum Corporation of America, BWW, August 24, 1970.

43. L. Luyckx, J. R. Bell, A. McLean and M. Korchynsky, "Sulfide Shape Control in High Strength Low Alloy Steels," 1970 AIME Session on 17-Thermodynamics and Kinetics-1, Denver, Colorado, February 17, 1969.

44. Ya. E. Col'dshtein, V. I. Zel'dovich, A. I. Komissarov, E. L. Lorotkevich, "Effect of Rare Earth Metals on the Properties of Chromium-Nickel Steel," Stal' 23, (4), 354-8, 1963; Eng. Trans., Stal' in English 23, 306-9, 1963.

45. "The Effect of Rare Earth Metals on the Properties of Steel Containing Carbon 0.4% and Steels Containing Carbon 0.4% with Nickel and Chromium," Anonymous, Sbornik Trudy Tsentr, Nauchn-issled. Inst. Chermoi Met., 1965, (39), 5-15; Met. Abstr., k, 720, 1966.

46. E. I. Nilolaev, Yu, V. Krykovskii, E. I. Tyurin, V. I. Yanoiskii, Chemical Heterogeneity and Nonmetallic Inclusions in Steel Ingots Containing Rare Earth Metals," Izv, VUZ-Chern, Met., 1965, (7), 37-42 Eng. Trans., H. Brutcher, No. 6626.

47. A. E. Korvosheev, B. V. Marinschenko and N. M. Fetisov, "Corrosion resistance of Cast Iron With and Without Additive Treatment," Russian Casting Production, March 1973.

48. W. F. Savage, "The Effect of Rare Earth Additions on Hydrogen-Induced Cracking in HY-80 Weldments," Presented at the International Symposium on Sulfide Inclusions in Steel," 7-8 November, 1974, Port Chester, N.Y.

49. D. G. Howden and P. A. Tews, "Hydrogen in HY-130 Weld Metal," Prepared for Office of Naval Research under Contract No. N00014-74-C-0407 (NR 031-770), July 31, 1975.

50. R. M. Vennett and G. S. Ansell, ASM Trans. Quarterly, Vol. 62, December 1969.

51. C. S. Kortovich, "Corrosion Fatigue Behavior of 4340 and D6AC Steels Below K_{Iscc}," Prepared for Office of Naval Research Under Contract N00014-69-C-0286, April 1974.

52. C. F. Barth and E. A. Steigerwald, "Evaluation of Hydrogen Embrittlement Mechanisms," Met. Trans. Vol. 1, December 1970, pp. 3451-3455.

53. H. H. Johnson, J. G. Morlet, and A. R. Troiano, Trans. TMS-AIME, 1958, Vol. 212, pp. 528-36.

54. A. M. Greene, "What Rare Earths Add to Steel," Iron Age, February 25, 1971.

55. Personal Communication with George Wade, Republic Steel Corporation, October 29, 1975.

56. W. G. Wilson and R. G. Wells, "Identifying Inclusions in Rare Earth Treated Steels," Metals Progress, December 1973.

57. A. R. Troiano, "The Role of Hydrogen and Other Interstitials in the Mechanical Behavior of Metals," ASM Trans., Vol. 52, 1960, pp. 54-80.

58. R. P. Wei, S. R. Novak and D. P. Williams, "Some Important Considerations in the Development of Stress Corrosion Cracking Test Methods," Materials Research and Standards, MTSRA, Vol. 12, No. 9, 1972.

Technical and Summary Reports

Organization	No. of Copies	Organization	No. of Copies
Defense Documentation Center Cameron Station Alexandria, Virginia 22314	(12)	Naval Air Propulsion Test Center Trenton, New Jersey 08628 Attn: Library	(1)
Office of Naval Research Department of the Navy		Naval Weapons Laboratory Dahlgren, Virginia 22448	
Attn: Code 471	(3)	Attn: Research Division	(1)
Code 105	(6)		
Code 470	(1)	Naval Construction Batallion Civil Engineering Laboratory Port Hueneme, California 93043	
Director Office of Naval Research Branch Office 495 Summer Street Boston, Massachusetts 02210	(1)	Attn: Materials Division	(1)
		Naval Electronics Laboratory Center San Diego, California 92152	
Director Office of Naval Research Branch Office 536 South Clark Street Chicago, Illinois 60605	(1)	Attn: Electronic Materials Sciences Division	(1)
		Naval Missile Center Materials Consultant Code 3312-1	
Office of Naval Research San Francisco Area Office 760 Market Street Room 447 San Francisco, California 94102	(1)	Point Mugu, California 93041	(1)
		Commanding Officer Naval Ordnance Laboratory White Oak Silver Spring, Maryland 20910	
Naval Research Laboratory Washington, D. C. 20390		Attn: Library	(1)
Attn: Code 6000	(1)	Naval Ship R&D Center Materials Department Annapolis, Maryland 21402	(1)
Code 6100	(1)		
Code 6300	(1)		
Code 6400	(1)	Naval Undersea Center San Diego, California 92132	
Code 2627	(6)	Attn: Library	(1)
Attn: Mr. F. S. Williams Naval Air Development Center Code 302 Warminster, Pennsylvania 18974	(1)	Naval Underwater System Center Newport, Rhode Island 02840 Attn: Library	(1)

Organization	No. Of Copies	Organization	No. of Copies
Naval Weapons Center China Lake, California 93555 Attn: Library	(1)	Commanding General Department of the Army Frankford Arsenal Philadelphia, Pennsylvania 19137 Attn: ORDBA-1320	(1)
Naval Postgraduate School Monterey, California 93940 Attn: Materials Sciences Dept.	(1)	Office of Scientific Research Department of the Air Force Washington, D. C. 20333 Attn: Solid State Div. (SRPS)	(1)

Naval Air Systems Command
Washington, D. C. 20360
 	
Attn: Code 52031
        Code 52032
        Code 320
	(1)
	(1)
	(1)
		Aerospace Research Labs
		Wright-Patterson AFB
		Building 450
		Dayton, Ohio 45433
			(1)

Naval Sea System Command Washington, D. C. 20362 Attn: Code 035	(1)	Air Force Materials Lab (LA) Wright-Patterson AFB Dayton, Ohio 45433	(1)
Naval Facilities Engineering Command Alexandria, Virginia 22331 Attn: Code 03	(1)	NASA Headquearters Washington, D. C. 20546 Attn: Code RRM	(1)
Scientific Advisor Commandant of the Marine Corps Washington, D. C. 20380 Attn: Code AX	(1)	NASA Lewis Research Center 21000 Brookpark Road Cleveland, Ohio 44135 Attn: Library	(1)

Naval Ship Engineering Center
Department of the Navy
Washington, D. C. 20360
Attn: Director, Materials
     Sciences
	(1)	National Bureau of Standards
		Washington, D. C. 20234
		
		Attn: Metallurgy Division (1)
		     Inorganic Materials Div.(1)	

Army Research Office Box CM, Duke Station Durham, North Carolina 27706 Attn: Metallurgy & Ceramics Div.	(1)	Atomic Energy Commission Washington, D. C. 20545 Attn: Metals & Materials Branch	(1)
Army Materials and Mechanics Research Center Watertown, Massachusetts 02172 Attn: Res. Programs Office (AMXMR-P)	(1)	Defense Metals & Ceramics Information Center Battelle Memorial Institute 505 King Avenue Columbus, Ohio 43201	(1)

Organization	No. of Copies	Organization	No. of Copies
Director Ordnance Research Laboratory P. O. Box 30 State College, Pennsylvania 16801	(1)		
Director Applied Physics Lab. University of Washington 1013 Northeast Fortieth Street Seattle, Washington 98105	(1)		
Metals and Ceramics Division Oak Ridge National Laboratory P. O. Box X Oak Ridge, Tennessee 37830	(1)		
Los Alamos Scientific Lab. P. O. Box 1663 Los Alamos, New Mexico 87544 Attn: Report Librarian	(1)		
Argonne National Laboratory Metallurgy Division P. O. Box 229 Lemont, Illinois 60439	(1)		
Brookhaven National Laboratory Technical Information Division Upton, Long Island New York 11973 Attn: Research Library	(1)		
Library Building 50 Room 134 Lawrence Radiation Laboratory Berkeley, California	(1)		

SUPPLEMENTARY DISTRIBUTION LIST

Technical and Summary Reports

Professor G. S. Ansell
Rensselaer Polytechnic Institute
Dept. of Metallurgical Engineering
Troy, NY   12181

Professor H. K. Birnbaum
University of Illinois
Department of Metallurgy
Urbana, IL   61801

Dr. E. M. Breinan
United Aircraft Corporation
United Aircraft Res. Laboratories
East Hartford, CT   06108

Professor H. D. Brody
University of Pittsburgh
School of Engineering
Pittsburgh, PA   15213

Professor J. B. Cohen
Northwestern University
Dept. of Material Sciences
Evanston, IL   60201

Professor M. Cohen
Massachusetts Institute of Technology
Department of Metallurgy
Cambridge, MA   02139

Professor B. C. Giessen
Northeastern University
Department of Chemistry
Boston, MA   02115

Dr. G. T. Hahn
Battelle Memorial Institute
Department of Metallurgy
505 King Avenue
Columbus, OH   43201

Professor R. W. Heckel
Carnegie-Mellon University
Schenley Park
Pittsburgh, PA   15213

Dr. David G. Howden
Battelle Memorial Institute
Columbus Laboratories
505 King Avenue
Columbus, OH   43201

Professor C. E. Jackson
Ohio State University
Dept. of Welding Engineering
190 West 19th Avenue
Columbus, OH   43210

Professor G. Judd
Rensselaer Polytechnic Institute
Dept. of Materials Engineering
Troy, NY   12181

Dr. C. S. Kortovich
TRW, Inc.
23555 Euclid Avenue
Cleveland, OH   44117

Professor D. A. Koss
Michigan Technological University
College of Engineering
Houghton, MI   49931

Professor A. Lawley
Drexel University
Dept. of Metallurgical Engineering
Philadelphia, PA   19104

Dr. H. Margolin
Polytechnic Institute of New York
333 Jay Street
Brooklyn, NY   11201

Professor K. Masabuchi
Massachusetts Institute of Technology
Department of Ocean Engineering
Cambridge, MA   02139

Dr. G. H. Meier
University of Pittsburgh
Dept. of Metallurgical and
  Materials Engineering
Pittsburgh, PA   15213

SUPPLEMENTARY DISTRIBUTION LIST (Cont'd)

Professor J. W. Morris, Jr.
University of California
College of Engineering
Berkeley, CA   94720

Professor K. Ono
University of California
Materials Department
Los Angeles, CA   90024

Professor W. F. Savage
Rensselaer Polytechnic Institute
School of Engineering
Troy, NY   12181

Dr. C. Shaw
Rockwell International Corp.
P.O. Box 1085
1049 Camino Dos Rios
Thousand Oaks, CA   91360

Professor O. D. Sherby
Stanford University
Materials Sciences Department
Stanford, CA   94300

Professor J. Shyne
Stanford University
Materials Sciences Department
Stanford, CA   94300

Dr. W. A. Spitzig
U.S. Steel Corporation
Research Laboratory
Monroeville, PA   15146

Dr. E. A. Starke, Jr.
Georgia Institute of Technology
School of Chemical Engineering
Atlanta, GA   30332

Professor N. S. Stoloff
Rensselaer Polytechnic Institute
School of Engineering
Troy, NY   12181

Dr. E. R. Thompson
United Aircraft Res. Laboratories
400 Main Street
East Hartford, CT   06108

Professor David Turnbull
Harvard University
Division of Engineering
   and Applied Physics
Cambridge, MA   02139

Dr. F. E. Wang
Naval Ordnance Laboratory
Physics Laboratory
White Oak
Silver Spring, MD   20910

Dr. J. C. Williams
Rockwell International
Science Center
P.O. Box 1085
Thousand Oaks, CA   91360

Professor H. G. F. Wilsdorf
University of Virginia
Department of Materials Science
Charlottesville, VA   22903

Dr. M. A. Wright
University of Tennessee
Space Institute
Department of Metallurgical
   Engineering
Tullahoma, TN   37388